









# Strigolactone deficiency induces jasmonate, sugar and flavonoid phytoalexin accumulation enhancing rice defense against the blast fungus *Pyricularia oryzae*

Zobaida Lahari<sup>1</sup> , Sarah van Boerdonk<sup>2</sup> , Olumide Owolabi Omoboye<sup>3,4</sup> , Michael Reichelt<sup>2</sup> ,  
Monica Höfte<sup>3</sup> , Jonathan Gershenzon<sup>2</sup> , Godelieve Gheysen<sup>1</sup>  and Chhana Ullah<sup>2</sup> 

<sup>1</sup>Department of Biotechnology, Ghent University, Ghent, 9000, Belgium; <sup>2</sup>Department of Biochemistry, Max Planck Institute for Chemical Ecology, Jena, 07745, Germany; <sup>3</sup>Department of Plants and Crops, Laboratory of Phytopathology, Ghent University, Ghent, 9000, Belgium; <sup>4</sup>Department of Microbiology, Faculty of Science, Obafemi Awolowo University, Ile-Ife, 220005, Nigeria

## Summary

Author for correspondence:

Chhana Ullah

Email: [cullah@ice.mpg.de](mailto:cullah@ice.mpg.de); [chhana.bd19@gmail.com](mailto:chhana.bd19@gmail.com)

Received: 22 November 2022

Accepted: 5 October 2023

*New Phytologist* (2024) **241**: 827–844

doi: 10.1111/nph.19354

**Key words:** flavonoid phytoalexins, glucose, jasmonic acid, *Magnaporthe oryzae*, plant defense signaling, plant–pathogen interactions, *rac-GR24*, sucrose.

- Strigolactones (SLs) are carotenoid-derived phytohormones that regulate plant growth and development. While root-secreted SLs are well-known to facilitate plant symbiosis with beneficial microbes, the role of SLs in plant interactions with pathogenic microbes remains largely unexplored.
- Using genetic and biochemical approaches, we demonstrate a negative role of SLs in rice (*Oryza sativa*) defense against the blast fungus *Pyricularia oryzae* (syn. *Magnaporthe oryzae*).
- We found that SL biosynthesis and perception mutants, and wild-type (WT) plants after chemical inhibition of SLs, were less susceptible to *P. oryzae*. Strigolactone deficiency also resulted in a higher accumulation of jasmonates, soluble sugars and flavonoid phytoalexins in rice leaves. Likewise, in response to *P. oryzae* infection, SL signaling was downregulated, while jasmonate and sugar content increased markedly. The *jar1* mutant unable to synthesize jasmonoyl-L-isoleucine, and the *coi1-18* RNAi line perturbed in jasmonate signaling, both accumulated lower levels of sugars. However, when WT seedlings were sprayed with glucose or sucrose, jasmonate accumulation increased, suggesting a reciprocal positive interplay between jasmonates and sugars. Finally, we showed that functional jasmonate signaling is necessary for SL deficiency to induce rice defense against *P. oryzae*.
- We conclude that a reduction in rice SL content reduces *P. oryzae* susceptibility by activating jasmonate and sugar signaling pathways, and flavonoid phytoalexin accumulation.

## Introduction

Strigolactones (SLs) are a relatively new class of plant hormones that regulate numerous processes, such as symbiosis with beneficial microorganisms (Akiyama *et al.*, 2005), inhibition of bud formation, shoot branching, tiller formation (Gomez-Roldan *et al.*, 2008; Umehara *et al.*, 2008) and root system architecture (López-Ráez *et al.*, 2017). Strigolactones have a strong connection to the rhizosphere with root-secreted SLs stimulating the germination of parasitic weed seeds (Cook *et al.*, 1966). Under inorganic phosphate deficiencies, plants increase their endogenous levels of SLs (Yoneyama *et al.*, 2012; Xi *et al.*, 2015), which are released into the rhizosphere to establish arbuscular mycorrhizal symbioses that provide the host plant with increased supplies of phosphate and other nutrients (Akiyama *et al.*, 2005; Kumar *et al.*, 2015; Das *et al.*, 2022).

The core SL biosynthetic pathway is well-conserved across the plant kingdom, and the key enzymes have been characterized

from many plants, including *Arabidopsis*, rice and pea (Mashiguchi *et al.*, 2021). Strigolactone synthesis starts in the plastid with the conversion of all-*trans*- $\beta$ -carotene into 9-*cis*- $\beta$ -carotene by the isomerase enzyme DWARF27 (D27) (Alder *et al.*, 2012). Following this, the common precursor for SLs, carlactone, is formed by two sequential reactions catalyzed by CAROTENOID CLEAVAGE DIOXYGENASE 7 (CCD7 or D17 or MAX3) and CCD8 (D10 or MAX4) with the formation of an intermediate product 9-*cis*- $\beta$ -apo-10'-carotenal (Mashiguchi *et al.*, 2021). Carlactone is then transported to the cytosol, where specific cytochrome P450 oxygenases such as MORE AXILLARY GROWTH1 (MAX1) and LATERAL BRANCHING OXIDOREDUCTASE (LBO) are responsible for various structural modifications. The highest quantities of SLs are thought to be produced in roots, and grafting experiments have confirmed root-to-shoot transport (Kameoka & Kyojuka, 2018). The presence of SLs at very low concentrations in plants, especially in leaves, and their structural diversity (> 30 natural SLs reported),

as well as the instability of some structures, make these signaling molecules challenging to detect and quantify. Like several other plant hormones, SL signaling relies on the ubiquitin-mediated proteasomal degradation of repressor proteins, involving a repressor called D53 (Mashiguchi *et al.*, 2021). DWARF14 (D14), a member of the  $\alpha/\beta$ -fold hydrolase superfamily with dual functions as a receptor and catalytic enzyme, plays a crucial role in SL signaling (Seto *et al.*, 2019) by physically interacting with SLs and undergoing a conformational change enabling the recruitment of D53 and the F-box protein MAX2, which results in the formation of a signaling complex with Skp1-Cullin-F-box (SCF). The resulting protein complex causes the polyubiquitination of D53, which is then degraded (Machin *et al.*, 2020). The proteasomal degradation of D53 allows transcriptional activation of SL-responsive genes (Omoarelojie *et al.*, 2019).

Strigolactones play essential roles in plant tolerance to various stresses. Among abiotic stresses, *Arabidopsis* mutants impaired in SL biosynthesis or signaling are hypersensitive to drought and salinity (Bu *et al.*, 2014; Ha *et al.*, 2014), with addition of exogenous SLs alleviating the deleterious effects of these stresses (N. Ma *et al.*, 2017; Wang *et al.*, 2019; Sattar *et al.*, 2022). Among biotic stresses, recent studies have provided some evidence that SLs are involved in plant–pathogen and plant–herbivore interactions (Torres-Vera *et al.*, 2014; Piisilä *et al.*, 2015; Decker *et al.*, 2017; Escudero Martinez *et al.*, 2019; Lahari *et al.*, 2019; Xu *et al.*, 2019; Li *et al.*, 2020). However, the roles of SLs in defenses against pathogens are highly variable depending on the plant species, organ of infection, stage of development and type of pathogen. For example, SLs were shown to enhance infection of the root-knot nematode *Meloidogyne graminicola* in rice (Lahari *et al.*, 2019), but reduce *M. incognita* infection in tomato roots (Xu *et al.*, 2019), even though in both cases SL signaling was induced in response to infection. Adding *rac*-GR24, a synthetic SL, to the culture media of several fungal root and leaf pathogens and endophytes resulted in effects ranging from nothing to strong growth inhibitions (Steinkellner *et al.*, 2007; Dor *et al.*, 2011). In *Arabidopsis*, SL mutants were found to be more susceptible to biotrophic pathogens, such as *Pseudomonas syringae* DC3000 and *Rhodococcus fascians* than necrotrophic pathogens (Stes *et al.*, 2015; Kalliola *et al.*, 2020). However, in tomato, the SL mutant *Slced8* displayed increased susceptibility to necrotrophic leaf pathogens, including *Botrytis cinerea* and *Alternaria alternata* (Torres-Vera *et al.*, 2014). In pea, the SL pathway did not affect the colonization of the soil-borne oomycete *Pythium irregulare* at all (Blake *et al.*, 2016). Hence, further studies are needed to unravel the role of SLs in plant–pathogen interactions and determine the underlying molecular mechanisms.

Plant hormones often interact with each other resulting in a fine-tuning of plant responses to different environmental conditions. This is true for SLs as well (Omoarelojie *et al.*, 2019), and SL mutants of rice (Lahari *et al.*, 2019), tomato (Xu *et al.*, 2019) and *Nicotiana attenuata* (Li *et al.*, 2020) were all shown to constitutively accumulate jasmonic acid (JA) and its derivatives (collectively known as jasmonates). Jasmonates are well-known to respond to insect herbivores and necrotrophic pathogens (Wasternack &

Strnad, 2018; Ruan *et al.*, 2019). The biosynthesis of jasmonates starts in the chloroplast with the release of  $\alpha$ -linolenic acid from membrane lipids. After several steps, *cis*-(+)-12-oxo-phytodienoic acid (*cis*-OPDA) is formed and transported from the chloroplast to the peroxisome, where the remainder of the steps in JA formation occur. Subsequently, JA is transported to the cytosol and further modified or conjugated, forming various derivatives such as 12-OH-JA, the 12-*O*-glucoside, jasmonoyl-L-isoleucine (JA-Ile), 12-OH-JA-Ile and 12-COOH-JA-Ile (Wasternack & Hause, 2013; Guo *et al.*, 2018; Ruan *et al.*, 2019). Although JA-Ile is considered the most active form of jasmonates as perceived by the COI1 receptor (Fonseca *et al.*, 2009), other JA derivatives such as *cis*-OPDA, 12-OH-JA-Ile can also activate JA signaling (Monte *et al.*, 2018; Poudel *et al.*, 2019). Upon perception of jasmonates, complexes are formed between SCF-COI1 and the JAZ (jasmonate-ZIM-domain proteins) repressor proteins. Degradation of JAZs releases the positive regulator MYC2, activating downstream JA responses (Pauwels & Goossens, 2011). In rice, for example, the accumulation of antifungal flavonoids, such as naringenin and sakuranetin, is regulated by the MYC2-dependent JA signaling pathway (Ogawa *et al.*, 2017; Xu *et al.*, 2021).

Soluble sugars such as glucose, fructose and sucrose are not only the basic energy currency in plants, but also involved in regulating development. Recent studies have revealed that sugars negatively regulate SL-mediated plant responses. For instance, sucrose alleviates SL-mediated inhibition of axillary bud outgrowth in rose and pea (Bertheloot *et al.*, 2020), and glucose was shown to reduce SL-induced leaf senescence of rice and bamboo (Tian *et al.*, 2018; Takahashi *et al.*, 2021). In rice seedlings, sucrose inhibits the degradation of the repressor protein D53, which results in the downregulation of SL-responsive genes, and subsequently alleviates the SL-induced inhibition of tiller bud formation (Patil *et al.*, 2022). Soluble sugars also act as signaling molecules in plant–pathogen interactions. For instance, sucrose application was shown to induce several defense-related genes and reduced *Pyricularia oryzae* (syn. *Magnaporthe oryzae*) infection in rice leaves (Gómez-Ariza *et al.*, 2007; Tun *et al.*, 2023). However, whether SLs themselves have any influence on soluble sugar content is not known.

Here, we investigated the role of SLs in rice defense against the hemibiotrophic fungus *P. oryzae*, which causes a blast disease destroying up to 30% of rice yield world-wide (Dean *et al.*, 2012). First, we employed SL biosynthetic and signaling mutants, and wild-type (WT) seedlings where SL formation was inhibited and found increased resistance to *P. oryzae*. Next, we showed that SL deficiency in rice leaves led to a remarkable accumulation of jasmonates, soluble sugars and flavonoid phytoalexins. These results were corroborated by the downregulation of SL signaling and induction of jasmonates and sugars during infection of WT rice seedlings by *P. oryzae*. Direct manipulation of both jasmonates and sugars revealed that these two groups of metabolites exhibited reciprocal positive enhancement with a remarkable accumulation of flavonoid phytoalexins. Finally, we showed that an intact JA signaling pathway is required for SL-deficiency to induce rice defense against *P. oryzae*.

## Materials and Methods

### Plant materials and growth conditions

Seeds of the SL biosynthetic mutant *d10*, the SL signaling mutant *d14* and their corresponding WT (*Oryza sativa* cv Shiohari) were kindly provided by Professor Mikio Nakazono, Nagoya University, and Dr. Itsuro Takamura, Hokkaido University, Japan. The *Tos17*-insertion mutant of *jar1* (NC0364; <http://tos.nias.affrc.go.jp/>) was obtained from the Rice Genome Resource Center in Japan (Miyao *et al.*, 2003). *jar1* is deficient in JA-Ile production due to a mutation in the enzyme JA amido synthetase (JAR) (Riemann *et al.*, 2008). The *coi1-18* RNAi line is compromised in JA response (Yang *et al.*, 2012). Both *jar1* and *coi1-18* lines were in the Nipponbare background. Seeds of the WT *O. sativa* cv Nipponbare were supplied by the United States Department of Agriculture (USDA, GSOR-100). Seeds of all mutant and transgenic lines and WT Shiohari were multiplied at the glasshouse facilities of Ghent University. For experiments, seeds were germinated on moist filter papers placed in a Petri dish at 30°C for 4–5 d. Unless otherwise stated, rice seedlings were then transplanted to PVC tubes containing sand and absorbent polymer and fertilized as described previously (Lahari *et al.*, 2019).

### Fungal inoculation and disease assessment

The virulent blast fungus *Pyricularia oryzae* (isolate VT5M1; Prof. Monica Höfte, Ghent University, Belgium) was originally isolated from rice in Vietnam (Thuan *et al.*, 2006). The fungus was cultured on a complete medium (CM) (Talbot *et al.*, 1993) at 28°C for 6–8 d. Spores of 7-d-old fungal cultures were collected and suspended in 0.2% (w/v) gelatin to a final concentration of  $5 \times 10^4$  spores ml<sup>-1</sup>. Two-week-old transplanted rice seedlings were thoroughly sprayed with the spore suspension using a compressor-powered airbrush gun (Badger Airbrush model 150TM). Inoculated rice seedlings were then incubated for 22 h in a dark chamber with  $\geq 90\%$  relative humidity and  $25 \pm 5^\circ\text{C}$ . The plants were then transferred to the glasshouse for disease development and scored at 6 d post inoculation (dpi) by counting the number of sporulating (ellipsoid to round lesion with a gray center) and nonsporulating lesions on the second leaf (De Vleeschauwer *et al.*, 2006; Z. Ma *et al.*, 2017). Representative pictures of typical disease symptoms were taken at 6 dpi. Unless otherwise stated, infection levels in all cases were determined using eight seedlings grown in separate pots. All infection experiments were repeated twice. For the time point experiment, the WT rice seedlings (cv Shiohari) were grown for 2 wk and inoculated by the blast fungus *P. oryzae* VT5M1. Leaf samples from both infected and uninfected control plants were collected at 1, 3 and 6 dpi always at the same time of the day (13:00–14:00 h) to avoid diurnal variation. Each time, four biological replicates per treatment were harvested, and each biological replicate consisted of a pool of leaves of four to five seedlings grown in separate pots. Samples were immediately frozen in liquid nitrogen and stored at  $-80^\circ\text{C}$  until further use.

### Treatment with SL inhibitor followed by *P. oryzae* inoculation

The SL biosynthesis inhibitor TIS108 was purchased from Chiralix (Nijmegen, the Netherlands), and dissolved in absolute ethanol to make a 10 mM stock solution. The spray solution (3  $\mu\text{M}$ ) was prepared in distilled water containing 0.02% (v/v) Tween 20. Two-week-old transplanted rice seedlings were thoroughly sprayed with TIS108 until runoff. Similarly, the mock-treated plants were sprayed with solvent only. One day after treatment, leaf samples for chemical analyses were collected in five biological replicates, each consisting of three to four individual seedlings, always at the same time of the day (13:00–14:00 h) to avoid diurnal variation. In a separate experiment, one day after spraying with TIS108 or control solution, rice seedlings were inoculated with *P. oryzae* as described previously, to determine the infection levels at 6 dpi. In another experiment, 2-week-old seedlings of JA mutants and WT Nipponbare were treated with TIS108 or the control solution (mock). Plants from both groups were inoculated with *P. oryzae*, and infection levels were assessed at 6 dpi.

### Treatment with the SL analog *rac*-GR24, methyl jasmonate (MeJA) and soluble sugars

A series of experiments were conducted using *rac*-GR24, MeJA and soluble sugars, including the monosaccharide glucose and disaccharide sucrose. Two-week-old transplanted WT seedlings were sprayed with 0.1 and 5.0  $\mu\text{M}$  *rac*-GR24 (Chiralix), and the mock seedlings were sprayed with the solvent (0.001% acetone) only. After 1 d, leaf samples were harvested in five biological replicates, each consisting of three-to-four seedlings grown in separate pots under the conditions described earlier. For other experiments, germinated rice seedlings (two seedlings per pot) were grown in 2 l Rosen Töpfe (Pöppelmann, Teku, Lohne, Germany) containing glasshouse substrate (Klasmann-Deilmann, Geeste, Germany) in a climate chamber (26°C : 24°C, day : night temperature, 70% relative humidity, 12 h, day : night light cycle) with periodical fertilization using Hoagland's solution. Three-week-old rice seedlings were thoroughly sprayed with 200  $\mu\text{M}$  MeJA solution containing 0.02% (v/v) Tween 20 in distilled water until runoff. Mock-treated plants were sprayed with 0.02% Tween 20. A separate spraying experiment was conducted using soluble sugars. Glucose and sucrose (Sigma-Aldrich) were dissolved in distilled water containing 0.02% (v/v) Tween 20 in final concentrations of 0.05 and 0.2 M, respectively. Glucose and sucrose solutions were thoroughly sprayed onto rice shoots, and mock-treated plants were sprayed with 0.02% Tween 20 in water. Immediately after spraying, rice seedlings were covered by polyethylene terephthalate bags (Toppits Bratschlauch, Minden, Germany) that were opened from the top after 6 h. Leaf samples were harvested 24 h after spraying in four biological replicates, each consisting of four to six seedlings. Jasmonic acid mutants and WT plants used for jasmonate and sugar quantification were also grown under these conditions.

For the complementation experiment using *rac*-GR24, rice seedlings of WT and SL mutants (*d10* and *d14*) were grown for

2 wk in separate pots. Half of the seedlings from each line were sprayed with 0.1  $\mu\text{M}$  *rac*-GR24, and the remaining seedlings were treated with 0.001% acetone in water as a mock. One day after spraying, leaf samples were collected in three biological replicates, each consisting of four-to-six seedlings. Immediately after harvesting, all samples were frozen quickly in liquid nitrogen and stored at  $-80^{\circ}\text{C}$  until further use. In a separate experiment, WT, *d10* and *d14* seedlings were treated with 0.1  $\mu\text{M}$  *rac*-GR24 or solvent only as a mock treatment. After 1 d, all seedlings were inoculated with the blast fungus *P. oryzae* (isolate VT5M1). The development of sporulating and nonsporulating lesions were observed at 6 dpi, as described earlier.

### Extraction and quantification of jasmonates and flavonoid phytoalexins

Frozen rice leaves were ground manually in liquid nitrogen to a fine powder. Approximately 40 mg of fresh leaf tissue was extracted with 1 ml of analytical grade methanol containing 40 ng of  $\text{D}_6$ -JA (HPC Standards GmbH, Cunnorsdorf, Germany), 8 ng  $\text{D}_6$ -JA-Ile (HPC Standards GmbH) and 40 ng  $\text{D}_6$ -ABA (Toronto Research Chemicals, Toronto, ON, Canada) as internal standards. Then, the content was vortexed vigorously for 10 s, incubated at  $20^{\circ}\text{C}$  for 30 min with continuous mild agitation and then centrifuged for 5 min at 13 000  $g$  at  $4^{\circ}\text{C}$ . Approximately 950  $\mu\text{l}$  of the supernatant was transferred to a new microcentrifuge tube. The extracts were directly analyzed using liquid chromatography-tandem mass spectrometry (LC-MS/MS).

To quantify phytohormones, chromatography was performed on an Agilent 1260 high-performance liquid chromatography (HPLC) system (Agilent Technologies, Santa Clara, CA, USA) coupled to a QTRAP 6500 tandem mass spectrometer (Sciex, Darmstadt, Germany) equipped with a turbo spray ion source operated in negative ionization mode. Hormones were separated on a Zorbax Eclipse XDB-C18 column (1.8  $\mu\text{m}$ , 50 mm  $\times$  4.6 mm) at  $25^{\circ}\text{C}$ , with two mobile phases consisting of 0.05% (v/v) formic acid in MilliQ water and acetonitrile. The flow rate and the elution profile were similar to the method described by Ullah *et al.* (2022) (Supporting Information Table S1). The parent ion and selected fragment ions of jasmonates were analyzed by multiple reaction monitoring (MRM) (Table S2). The collected mass data were processed using the ANALYST 1.6 software (Applied Biosystems, Darmstadt, Germany). The absolute concentrations of JA and JA-Ile were determined by comparison with the internal standards  $\text{D}_6$ -JA and  $\text{D}_6$ -JA-Ile, respectively. Relative concentrations of *cis*-OPDA and OH-JA were determined using  $\text{D}_6$ -JA applying an experimental response factor of 1.0. Relative levels of OH-JA-Ile and COOH-JA-Ile were quantified using  $\text{D}_6$ -JA-Ile, applying an experimental response factor of 1.0.

To quantify flavonoid phytoalexins, the 1260 HPLC-QTRAP 6500 mass spectrometer system equipped with a turbo spray ion source was operated in positive ionization mode. Targeted metabolites were separated using the Zorbax Eclipse XDB-C18 column at  $25^{\circ}\text{C}$ , with two mobile phases consisting of 0.05% (v/v) formic acid in MilliQ water and acetonitrile as mobile phases A and B, respectively. The flow rate was  $1.0\text{ ml min}^{-1}$  with a

gradient over 12.0 min (Table S3). The parent ion and selected fragment ions of naringenin, sakuranetin and the internal standard  $\text{D}_6$ -ABA were analyzed by MRM (Table S4). The collected mass data were processed using the software MULTIQUANT 3.0.3 (Sciex). The concentrations of naringenin and sakuranetin were determined by comparison with  $\text{D}_6$ -ABA, applying the experimental response factors of 0.77 and 0.51, respectively.

### Quantification of reactive oxygen species (ROS)

Hydrogen peroxide ( $\text{H}_2\text{O}_2$ ) from leaf tissues was quantified using Amplex<sup>®</sup> Red Hydrogen Peroxide Assay Kit (Invitrogen) following the method described by Chakraborty *et al.* (2016) with some modification. Briefly,  $50 \pm 2$  mg of homogenized leaf tissue was extracted in 500  $\mu\text{l}$  sodium phosphate buffer (pH 7.4). Samples were vigorously vortexed, and then incubated for 30 min at  $20^{\circ}\text{C}$  with mild agitation. Following centrifugation for 5 min at 12 000  $g$  and  $20^{\circ}\text{C}$ , 300  $\mu\text{l}$  of supernatant was transferred to a new eppendorf tube, and samples were placed on ice until analysis. To quantify  $\text{H}_2\text{O}_2$  concentration, 47  $\mu\text{l}$  of the sodium phosphate buffer, 50  $\mu\text{l}$  of the Amplex Red Reagent Cocktail (horseradish peroxidase and the Amplex Red Reagent) and 3  $\mu\text{l}$  of fresh tissue extract were added to each well of a flat bottom 96-well plate (Greiner Bio-One, Frickenhausen, Germany) followed by a gentle mix using the pipette. The plate was covered immediately with aluminum foil to protect the contents from light, gently shaken at room temperature for 10 min and incubated for an additional 20 min without shaking. Fluorescence of the product Resorufin was measured using  $560 \pm 10$  nm excitation and  $590 \pm 10$  nm emission filters using an Infinite 200 Fluorescence Microplate Reader (Tecan, Maennendorf, Switzerland). All standards and samples were run with two technical replicates.  $\text{H}_2\text{O}_2$  concentrations were calculated using a standard curve run on the same plate, including appropriate blanks.

### Sugar quantification using LC-MS/MS

To analyze soluble sugars, the methanol tissue extracts were diluted 1 : 10 in Milli-Q water containing  $^{13}\text{C}$ -glucose (Sigma-Aldrich) and  $^{13}\text{C}$ -fructose (Toronto Research Chemicals) as internal standards with a concentration of  $5\text{ }\mu\text{g ml}^{-1}$ . Sugars were analyzed using an Agilent 1200 HPLC system equipped with an API3200 tandem mass spectrometer. The HPLC was equipped with a hydrophilic interaction liquid chromatography (HILIC) column (apHera-NH2 Polymer; Supelco, Bellefonte, PA, USA), and chromatographic separation was performed using water and acetonitrile as mobile phases A and B, respectively, with a flow rate of  $1.0\text{ ml min}^{-1}$  (Table S5). The mass spectrometer equipped with a turbo spray ion source was operated in the negative ionization mode (Ullah *et al.*, 2022). Multiple reaction monitoring was used to monitor selected parent ion to product ion formation for each analyte (Table S6). Standards of sucrose (Sigma-Aldrich) and raffinose (Fluka, Seelze, Germany) were used to prepare external standard curves. Data were acquired using the software ANALYST 1.6, and quantification was performed using the software MULTIQUANT 3.0.3 (Sciex). The concentrations of glucose and fructose were

determined relative to the internal standards of  $^{13}\text{C}$ -glucose and  $^{13}\text{C}$ -fructose, respectively. The contents of sucrose and raffinose were calculated based on external standard curves.

### RNA extraction, complementary DNA (cDNA) synthesis and RT-qPCR

Total RNA was isolated from *c.* 50 mg of finely ground leaf tissues using the Invitrap Spin Plant RNA Mini Kit (Stratec Biomedical,

Birkenfeld, Germany) following the manufacturer's instructions, except that an additional DNase treatment was included using a Qiagen RNase-Free DNase Set as described by Ullah *et al.* (2017). Reverse transcription (RT) of 1  $\mu\text{g}$  total RNA into cDNA was achieved by using SuperScript III reverse transcriptase (Invitrogen) and 50 pmol Oligo (dT)12-18 Primer (Invitrogen) in a reaction volume of 20  $\mu\text{l}$  following the manufacturer's instructions. RT-qPCR reactions were performed in a 20  $\mu\text{l}$  volume containing 10  $\mu\text{l}$  Brilliant III Ultra-Fast SYBR Green QPCR Master Mix

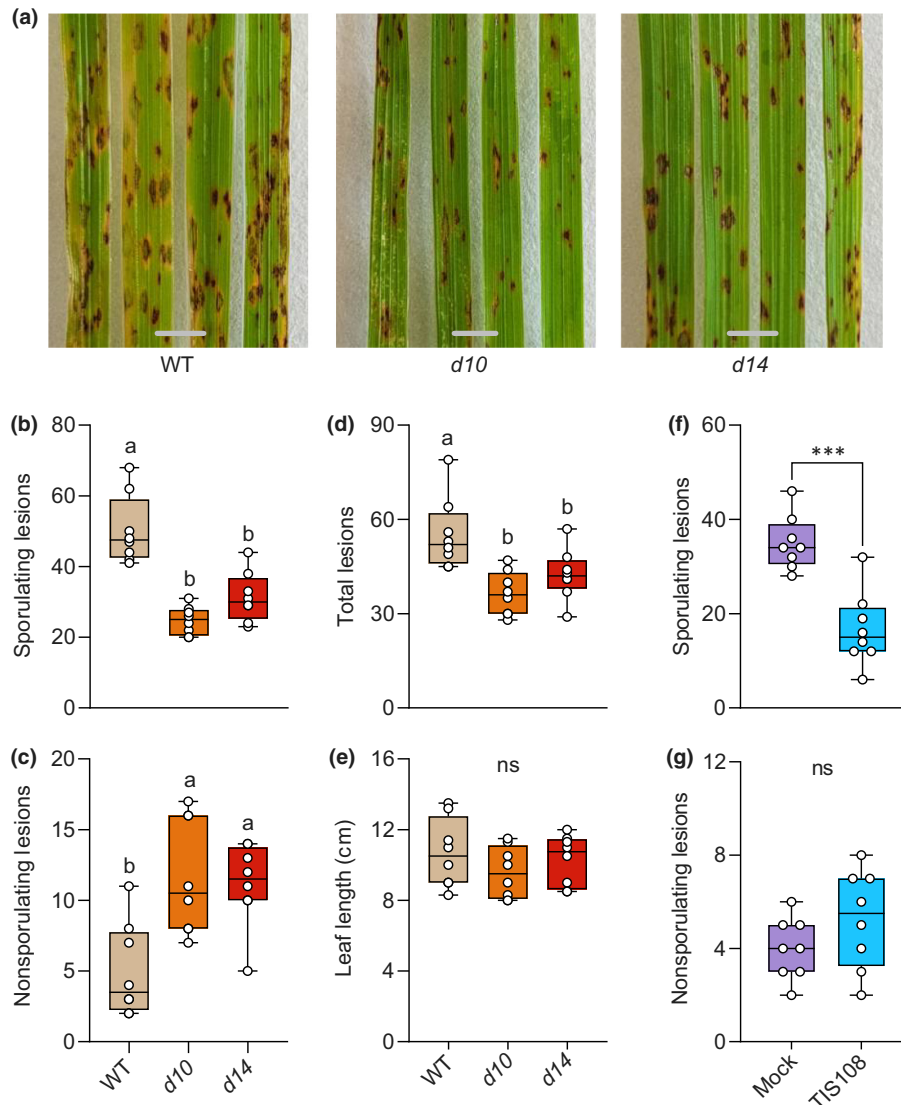


**Fig. 1** Strigolactone (SL) deficiency in rice reduces infection by the leaf blast fungus *Pyricularia oryzae*. (a–e) Rice mutants in SL biosynthesis and signaling were less susceptible to *P. oryzae*. Two-week-old transplanted rice seedlings were inoculated with the *P. oryzae* strain VT5M1 by spraying a spore suspension, and the disease was scored at 6 d post inoculation (dpi). (a) Representative photographs show blast disease symptoms on leaves of wild-type (WT) Shiokari, the SL-biosynthetic mutant *d10* and the SL-signaling mutant *d14*. Bars, 5 mm. Average number of (b) sporulating, (c) nonsporulating and (d) total lesions on the second youngest leaf. Data were analyzed using a one-way ANOVA, followed by Tukey's multiple comparison test with a 95% confidence interval. Different letters above box plots indicate groups that are significantly different ( $P < 0.05$ ). (e) Average length of the second youngest leaf used for disease scoring. Data were analyzed using a one-way ANOVA ( $P = 0.412$ , ns, nonsignificant). (f, g) Pretreatment with the SL biosynthesis inhibitor TIS108 reduced *P. oryzae* infection in rice leaves. Two-week-old transplanted rice seedlings of WT Shiokari were sprayed with TIS108 or with solvent only as a mock control. One day after spraying, seedlings were inoculated with the leaf blast fungus *P. oryzae*, and the disease severity was scored at 6 dpi. Average number of (f) sporulating and (g) nonsporulating lesions on the second youngest leaf. Data were analyzed using a two-tailed *t*-test (\*\*\*,  $P < 0.001$ ; ns, nonsignificant). Each box (b–g) extends from the 25<sup>th</sup> to the 75<sup>th</sup> percentiles, and the horizontal line inside the box represents the median. Whiskers were plotted down to the minimum and up to the maximum value, and all data points are shown on the graph as open circles ( $n = 8$ ).

(Agilent Technologies), 10 pmol forward and 10 pmol reverse primers, and template cDNA. Reactions were performed using a CFX Connect Real-Time PCR Detection System (Bio-Rad) using a two-step amplification protocol (Lahari *et al.*, 2019). Transcript abundance was calculated from four biological replicates per treatment, with each biological sample consisting of three technical replicates, and was normalized to the abundance of the housekeeping genes *OsExp* and *OsActin*. The gene-specific primer sequences are provided in Table S7.

### Statistical analyses

Statistical analyses were performed using GRAPHPAD PRISM v.9.5.1 and R-statistical package R 4.2.2. First, the normality and variance of each dataset were checked using Shapiro–Wilk and Levene tests, respectively. Whenever necessary, data were transformed using square root or  $\log_{10}$  to fulfill the assumptions for parametric tests. Normally distributed data were then analyzed by analysis of variance (ANOVA) or two-tailed Student's *t*-tests. In the case of ANOVA, Tukey's multiple comparisons *post hoc* test was performed. Statistical significances of *t*-test and ANOVA (\*,  $P < 0.05$ ; \*\*,  $P < 0.01$ ; \*\*\*,  $P < 0.001$ ) are provided in respective figures or figure legends. Statistical results of two-way ANOVAs are provided in Tables S8–S13. The schematic model (Fig. 9) was created using BIORENDER (<https://app.biorender.com>).

## Results

### SL biosynthetic and signaling mutants are less susceptible to *P. oryzae*

To investigate whether SLs are involved in regulating rice susceptibility to the blast fungus *P. oryzae*, we conducted an infection experiment using the SL biosynthetic mutant *d10*, the SL perception mutant *d14* and their corresponding WT line (cv Shiokari). Both *d10* and *d14* mutants were found to be less susceptible to the blast fungus *P. oryzae* VT5M1 than the WT (Fig. 1a). To estimate the disease severity on these lines, we categorized different lesion types on the second leaf from the top, as described previously (De Vleeschauwer *et al.*, 2006; Z. Ma *et al.*, 2017). The number of sporulating lesions, characterized by an ellipsoid to round shape with a gray center, was significantly higher on WT leaves than on the mutants (Fig. 1b). On the contrary, nonsporulating lesion numbers were slightly higher on the mutants (Fig. 1c). Total lesion numbers, dominated by the sporulating lesions, were also significantly higher on WT plants (Fig. 1d). While *c.* 90% of the total lesions contained spores on WT, only 55–60% of lesions developed into sporulating lesions in both *d10* and *d14* mutants (Fig. S1). The average length of the second youngest leaf did not vary between the mutants and WT plants at the time of fungal infection (Fig. 1e). Taken together, reduced susceptibility of the rice *d10* and *d14* mutants to *P. oryzae* suggests that the loss-of-function of SLs contributes to reduced blast severity in leaves.

To further determine the effect of SL deficiency on rice susceptibility against *P. oryzae*, we treated 2-wk-old WT rice seedlings (cv Shiokari) with TIS108, an inhibitor of SL biosynthesis

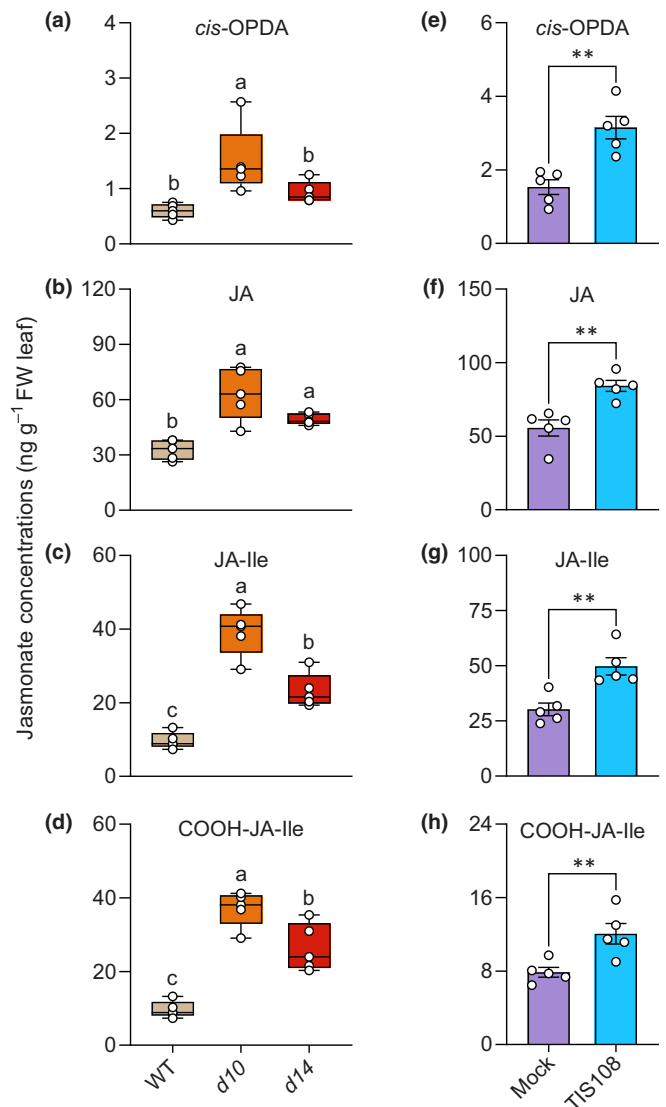


**Fig. 2** Strigolactone (SL) deficiency induces jasmonate accumulation in rice leaves. (a–d) Increased accumulation of jasmonates in SL biosynthetic (*d10*) and SL signaling (*d14*) mutants. Shoots of transplanted 2-week-old rice seedlings were harvested in five biological replicates, each consisting of a pool of three-to-four seedlings grown in separate pots. Hormone levels were measured using a triple quadrupole mass spectrometer. Data were analyzed using a one-way ANOVA, followed by Tukey's multiple comparison test with a 95% confidence interval. Different letters above box plots indicate groups that are significantly different ( $P < 0.05$ ). Each box extends from the 25<sup>th</sup> to the 75<sup>th</sup> percentiles, and the horizontal line inside the box represents the median. Whiskers were plotted down to the minimum and up to the maximum value, and all data points are shown on the graph as open circles ( $n = 5$ ). (e–h) Enhanced accumulation of jasmonates in wild-type (WT) (cv Shiokari) rice seedlings after treatment with the SL biosynthesis inhibitor TIS108. Two-week-old rice seedlings were treated with 3  $\mu\text{M}$  TIS108 or solvent only as control (mock), and leaf samples were harvested after 24 h in five biological replicates, each consisting of a pool of three-to-four seedlings grown in separate pots. Jasmonate data were analyzed using a two-tailed *t*-test (\*\*,  $P < 0.01$ ). Data are presented as the mean  $\pm$  SE, and all data points are shown on the graph as open circles ( $n = 5$ ). *cis*-OPDA, *cis*(+)-12-oxo-phytodienoic acid; COOH-JA-Ile, 12-carboxy-jasmonoyl-isoleucine; JA, jasmonic acid; JA-Ile, jasmonoyl-isoleucine.

(Ito *et al.*, 2011), or with solvent only as a control (mock). One day after spraying, both mock and SL-inhibited seedlings were inoculated with *P. oryzae* VT5M1, and disease development was recorded 6 d after fungal inoculation. TIS108-treated leaves showed a significantly lower number of sporulating lesions by *c.* 50% than the mock control (Fig. 1f). A few nonsporulating lesions were also found on both mock- and TIS108-treated seedlings, but the numbers were not statistically different (Fig. 1g). TIS108 had no direct toxic effects on *P. oryzae* (Fig. S2). These results further validate that the loss-of-function of SLs in rice leaves reduced the blast severity caused by the fungus *P. oryzae*.

### Loss-of-function of SLs promotes jasmonate and sugar accumulation in rice leaves

Previously, we reported that several rice SL mutants accumulate elevated levels of jasmonates in their roots compared with WT plants (Lahari *et al.*, 2019). To determine whether the leaves of these mutants also accumulate higher levels of jasmonates, we analyzed the concentrations of JA metabolites in the leaves of 2-week-old rice seedlings. Concentrations of *cis*(+)-12-oxophytodienoic acid (*cis*-OPDA), a precursor of JA, were significantly higher in the SL biosynthetic mutant *d10* than in the WT (Fig. 2a). Content of JA was significantly higher in the leaves of both *d10* and *d14* than in the WT leaves (Fig. 2b). Similarly, levels of jasmonoyl-L-isoleucine (JA-Ile) and 12-carboxy-jasmonoyl-isoleucine (COOH-JA-Ile) were significantly higher in both SL biosynthetic and signaling mutants than in WT (Fig. 2c,d). Next, we quantified jasmonate content in leaves of the WT Shiohari with or without the application of the SL biosynthetic inhibitor TIS108. Inhibition of SL biosynthesis resulted in increased accumulation of *cis*-OPDA, JA, JA-Ile and COOH-JA-Ile (Fig. 2e–h). We also treated WT rice seedlings with the synthetic SL *rac*-GR24, at low and high concentrations. One day after treatment, levels of jasmonates, especially the most active form JA-Ile, decreased significantly in leaves compared to the control (Fig. S3). Furthermore, exogenous *rac*-GR24 restored the basal levels of JA and JA-Ile in the SL biosynthetic mutant *d10*, while the SL signaling mutant *d14* was not responsive (Fig. S4). Together, our data indicate that SLs negatively regulate the accumulation of jasmonates in rice leaves.

Soluble sugars are known to antagonize the functions of SLs in different plants, including rice (Barbier *et al.*, 2015; Wang *et al.*, 2020; Patil *et al.*, 2022). Whether SLs also have a similar negative effect on sugar concentrations is not known. Because soluble sugars were shown to promote rice defense against *P. oryzae* (Gómez-Ariza *et al.*, 2007; Tun *et al.*, 2023), we hypothesized that enhanced resistance due to SL deficiency could also be linked to sugar content. Therefore, we quantified soluble sugar concentrations in the rice SL mutants using LC–MS/MS and compared them with the WT Shiohari. The levels of the monosaccharides glucose and fructose were similar in both mutants and WT seedlings (Fig. 3a). By contrast, both SL biosynthetic and signaling mutants accumulated significantly higher amounts of the disaccharide sucrose and the trisaccharide raffinose than WT plants (Fig. 3a). To further validate the negative

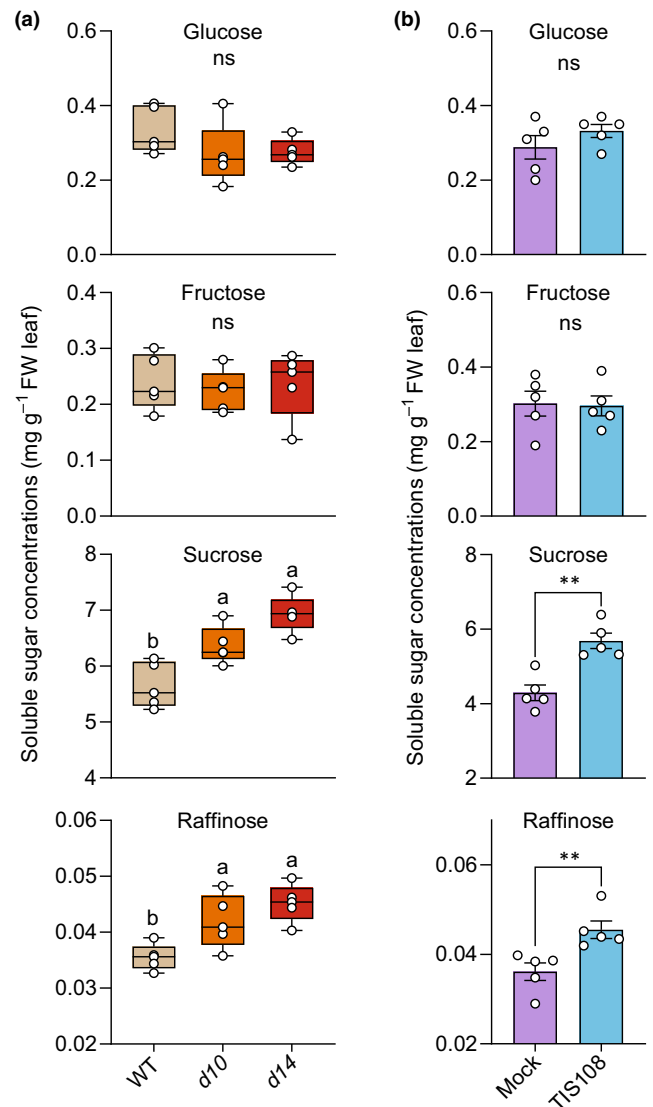


**Fig. 3** Strigolactone (SL) deficiency increases soluble sugar content in rice leaves. (a) Levels of soluble sugars in SL biosynthetic (*d10*) and SL signaling (*d14*) mutants. Leaves of 2-wk-old rice seedlings were harvested in five biological replicates, each consisting of a pool of three-to-four seedlings grown in separate pots. Concentrations of soluble sugars were determined using a triple quadrupole mass spectrometer. Data were analyzed using a one-way ANOVA, followed by Tukey's multiple comparisons test with a 95% confidence interval. Different letters above box plots indicate groups that are significantly different ( $P < 0.05$ ). Each box extends from the 25<sup>th</sup> to the 75<sup>th</sup> percentiles, and the horizontal line inside the box represents the median. Whiskers were plotted down to the minimum and up to the maximum value, and all data points are shown on the graph as open circles ( $n = 5$ ). (b) Accumulation of sugars in the leaves of rice seedlings after treatment with the SL-biosynthetic inhibitor TIS108. Two-week-old wild-type (WT) (cv Shiohari) rice seedlings were sprayed with TIS108 in aqueous solution with 0.001% ethanol and 0.02% Tween 20 or with ethanol and Tween 20 only as a mock control. Leaf samples were harvested after 24 h of treatment in five biological replicates, each consisting of a pool of three-to-four seedlings grown in separate pots. Data were analyzed using a two-tailed *t*-test (\*\*,  $P < 0.01$ ; ns, nonsignificant). Data are presented using bar plots as the mean  $\pm$  SE, and all data points are shown on the graph as open circles ( $n = 5$ ).

consequence of SLs on soluble sugar concentrations, we inhibited the SL biosynthesis in WT Shiokari using TIS108. The soluble sugar concentrations were analyzed after 24 h of treatment. Concentrations of both glucose and fructose did not change in TIS108-treated rice seedlings (Fig. 3b). However, we found a significant increase in sucrose and raffinose content in rice leaves treated with TIS108 (Fig. 3b). By contrast, rice seedlings treated with *rac*-GR24 exhibited significantly reduced leaf sugar concentrations, including those of glucose, fructose and sucrose (Fig. S5). Taken together, analyses of SL mutants, WT seedlings after treatment with the SL inhibitor TIS108 and SL analogue *rac*-GR24 suggest that inhibition of the SL signaling pathway induces the accumulation of soluble sugars and jasmonates.

Reactive oxygen species play dual roles during compatible interactions between rice and the blast fungus *P. oryzae* (Kou *et al.*, 2019). During the early stages of infection by virulent *P. oryzae*, transient ROS accumulation is necessary for appressorium formation and penetration. At the same time, the host-derived ROS needs to be neutralized by the fungus at the later stages of infection to circumvent rice defense (Kou *et al.*, 2019). To investigate whether ROS concentrations differ in SL-mutants during the commencement of *P. oryzae* infection, we quantified the content of H<sub>2</sub>O<sub>2</sub> using the Amplex Red assay. Levels of

H<sub>2</sub>O<sub>2</sub> were found to be similar in WT plants and in SL biosynthetic and signaling *d*-mutants (Fig. S6a). We also quantified ROS content in the leaves of WT seedlings after treatment with TIS108 and compared them with the untreated control. Levels of H<sub>2</sub>O<sub>2</sub> did not change after treatment with the SL inhibitor (Fig. S6b). Furthermore, we treated WT rice seedlings with *rac*-GR24 and quantified ROS content after 24 h. Reactive oxygen species concentrations did not change after treatment with 0.1 μM GR24, while a decrease in ROS content was observed in seedlings treated with a 50-fold higher dose of *rac*-GR24 (Fig. S7). These results suggest that elevated defense in SL mutants and TIS108-treated WT plants against *P. oryzae* is unlikely to be associated with oxidative stress in rice leaves.

#### Levels of jasmonates and soluble sugars increase in *P. oryzae*-infected leaves with downregulation of the SL signaling pathway

In order to determine the temporal changes in jasmonate content in leaves after infection by the blast fungus *P. oryzae*, a time-course experiment was conducted using the WT rice cultivar Shiokari. Concentrations of jasmonates did not change 1 d after *P. oryzae* inoculation (Fig. 4). At 3 dpi, *cis*-OPDA, a precursor of JA,

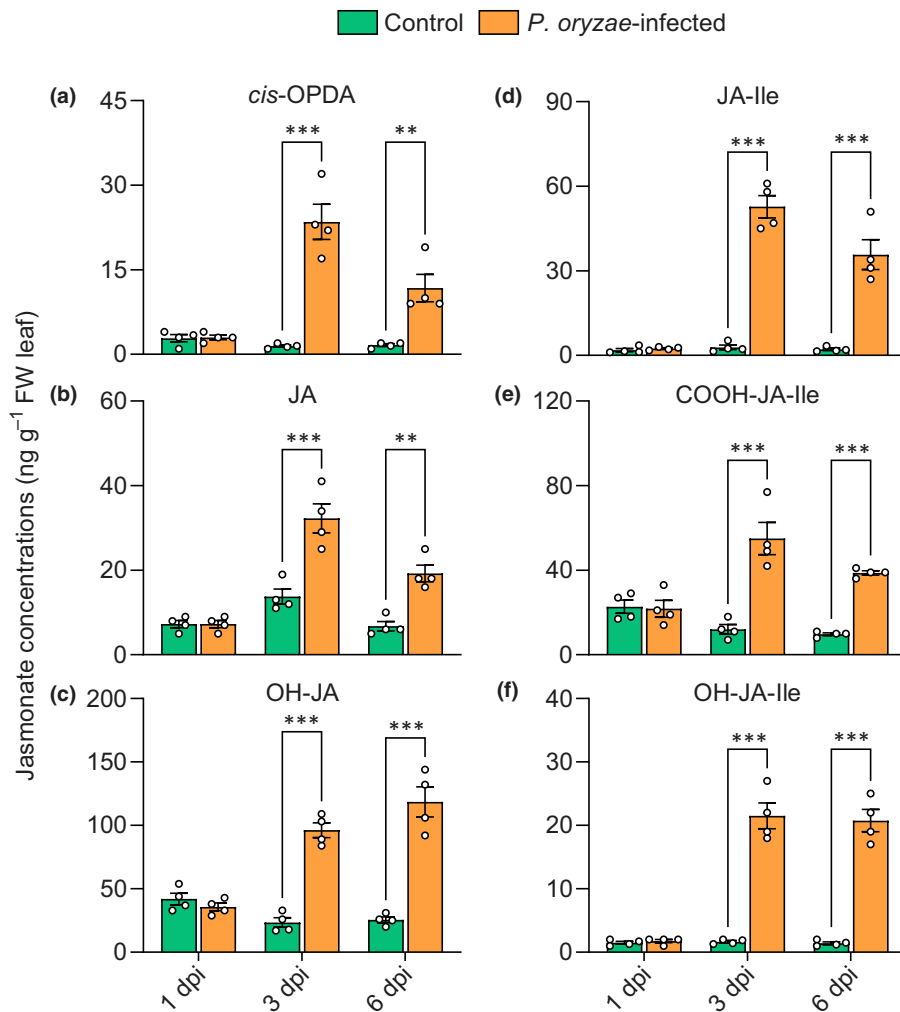


**Fig. 4** Induction of jasmonates in rice leaves in response to *Pyricularia oryzae* infection. Two-week-old rice seedlings were inoculated with the fungus *P. oryzae*, and the control seedlings were sprayed with solvent (0.2% gelatin in water) only. Leaf samples were harvested at 1, 3 and 6 d post inoculation (dpi) in four biological replicates, each consisting of a pool of four-to-five seedlings grown in separate pots. Concentrations of (a) *cis*-OPDA, (b) JA, (c) OH-JA, (d) JA-Ile, (e) COOH-JA-Ile, and (f) OH-JA-Ile were determined using a triple quadrupole mass spectrometer. Jasmonate data were analyzed using a two-way ANOVA, followed by Tukey's multiple comparison test with a 95% confidence interval. Statistical details of a two-way ANOVA for the levels of jasmonic acid (JA) metabolites are provided in Supporting Information Table S8. Significantly different comparisons between control vs infected levels at each time point are displayed on graphs using asterisks (\*\*,  $P < 0.01$ ; \*\*\*,  $P < 0.001$ ). Data are presented as the mean  $\pm$  SE, and all data points are shown on the graph as open circles ( $n = 4$ ). *cis*-OPDA, *cis*-(+)-12-oxo-phytodienoic acid; COOH-JA-Ile, 12-carboxy-JA-Ile; JA, jasmonic acid; JA-Ile, jasmonoyl-isoleucine; OH-JA, hydroxy-JA; OH-JA-Ile, 12-hydroxy-JA-Ile.

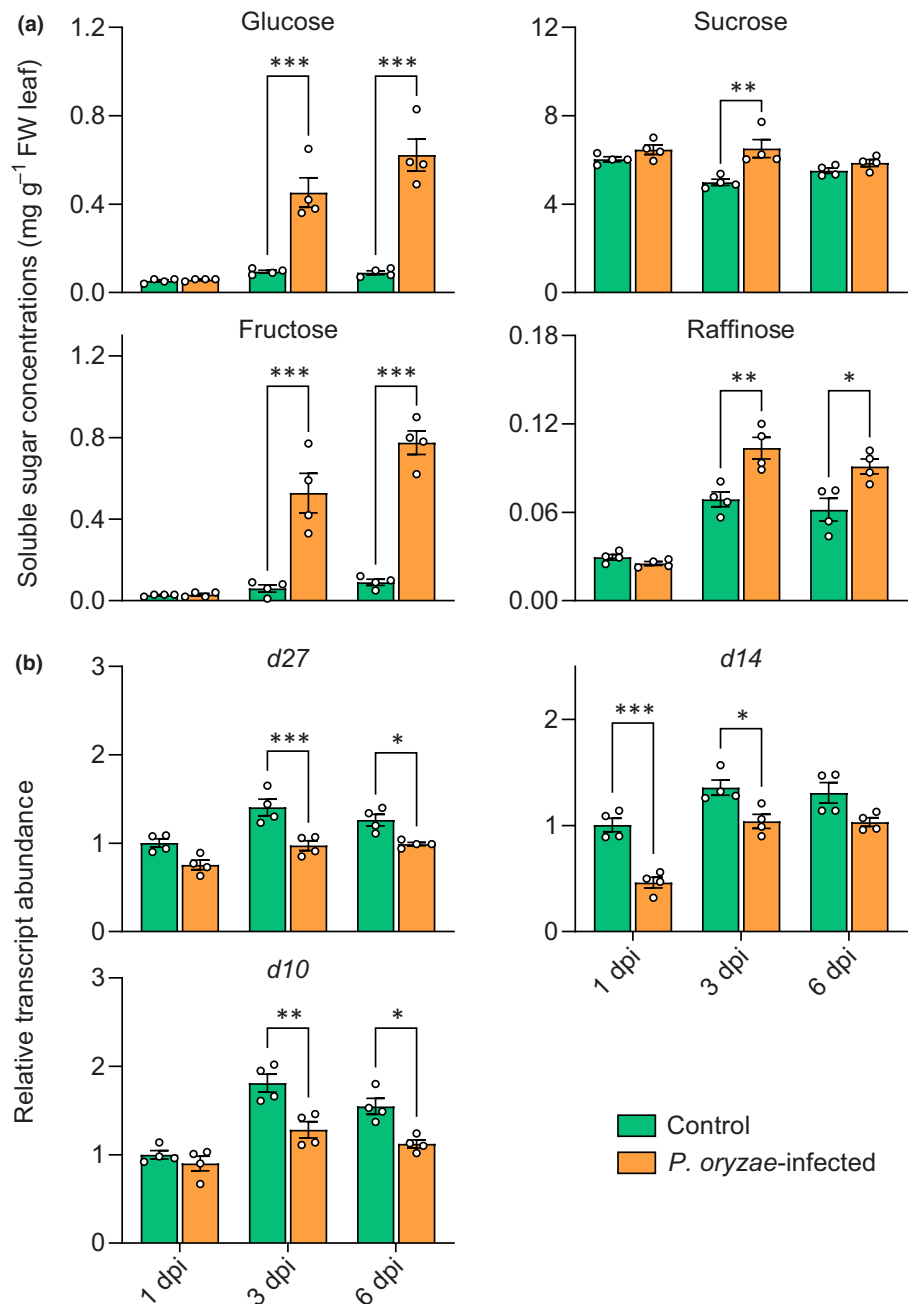


increased *c.* 16-fold after fungal infection compared with control leaves, while a seven-fold increase was found at 6 dpi (Fig. 4a). Similarly, JA levels were two- to three-fold higher in *P. oryzae*-infected leaves than in the corresponding controls at 3 and 6 dpi (Fig. 4b). A sustained accumulation of OH-JA was found at 3 and 6 dpi (Fig. 4c). JA-Ile, considered the most bioactive metabolite in the jasmonate pathway (Fonseca *et al.*, 2009), was also induced at levels up to 30-fold in response to infection by the blast fungus at 3 and 6 dpi (Fig. 4d). Similarly, concentrations of the JA-Ile derivatives, including COOH-JA-Ile and OH-JA-Ile, were significantly higher in *P. oryzae*-colonized rice leaves at 3 and 6 dpi than in the corresponding controls (Fig. 4e,f). The marked accumulation of jasmonates, including a JA precursor, active forms and

catabolites, suggests that rice seedlings induce the JA biosynthetic pathway in their leaves in response to *P. oryzae* infection.

Next, we quantified soluble sugar concentrations in *P. oryzae*-infected and corresponding control leaves. Levels of the monosaccharides, including glucose and fructose, increased remarkably after fungal colonization at 3 and 6 dpi (Fig. 5a). The content of the disaccharide sucrose was slightly higher in *P. oryzae*-infected plants at 3 dpi, while the basal levels were maintained at 1 and 6 dpi (Fig. 5a). The levels of raffinose, a trisaccharide, increased significantly in *P. oryzae*-infected plants at 3 and 6 dpi compared to controls (Fig. 5a). These results suggest that rice seedlings increase soluble sugar and jasmonate levels in response to *P. oryzae* infection.

**Fig. 5** Changes in soluble sugar content and transcripts of strigolactone (SL) genes in response to *Pyricularia oryzae* infection. (a) Accumulation of soluble sugars and (b) downregulation of the SL genes in rice leaves after *P. oryzae* infection. Samples from both fungal-infected and control leaves were harvested at 1, 3 and 6 d post inoculation (dpi) in four biological replicates, each consisting of a pool of four-to-five seedlings grown in separate pots. Soluble sugar concentrations were quantified using a triple quadrupole mass spectrometer. Relative transcripts of the SL biosynthetic (*d27* and *d10*) and signaling (*d14*) genes were determined using RT-qPCR and normalized to the transcript levels of the housekeeping genes *OsExp* and *OsActin*. Data were analyzed using a two-way ANOVA, followed by Tukey's multiple comparison test with a 95% confidence interval. Statistical details of a two-way ANOVA for the levels of sugar metabolites and SL gene transcripts are provided in Supporting Information Tables S9 and S10. Significantly different comparisons between control vs *P. oryzae*-infected rice leaves at each time point are displayed on graphs using asterisks (\*,  $P < 0.05$ ; \*\*,  $P < 0.01$ ; \*\*\*,  $P < 0.001$ ). Data are presented as the mean  $\pm$  SE, and all data points are shown on the graph as open circles ( $n = 4$ ).



To determine whether the SL pathway is altered in rice leaves inoculated with the blast fungus *P. oryzae*, we analyzed transcripts of two SL biosynthetic genes (*d27*, *d10*) and one signaling gene (*d14*) over the course of infection. The relative expression of *d27* was found to be slightly lower in *P. oryzae*-infected leaves than in control leaves at 1 dpi, and significantly lower transcripts were found on subsequent days of infection at 3 and 6 dpi than in the corresponding controls (Fig. 5b). Similarly, a significant downregulation of the biosynthetic gene *d10* was found after fungal infection at 3 and 6 dpi (Fig. 5b). Downregulation of the SL signaling gene *d14* was already found in *P. oryzae*-infected leaves at the earlier time points 1 and 3 dpi (Fig. 5b). Taken together, *P. oryzae* infection in rice leaves resulted in the rapid downregulation of the SL signaling pathway followed by concomitant accumulation of jasmonates and soluble sugars.

## SLs negatively regulate flavonoid phytoalexin accumulation in rice leaves

Rice is known to accumulate several classes of phytoalexins, including some classes of flavonoids. Previous studies have shown that the flavanone sakuranetin, a methoxy derivative of naringenin whose accumulation is regulated by JA signaling, is an effective antimicrobial metabolite against *P. oryzae* (Miyamoto *et al.*, 2016; Ogawa *et al.*, 2017). We asked whether SLs also regulate flavanone levels in rice leaves. First, we quantified the accumulation of naringenin and sakuranetin in rice leaves infected by *P. oryzae*. In response to blast infection, these antimicrobial metabolites were induced remarkably up to 535-fold at 3 dpi (Fig. 6a). Then, we quantified the levels of flavonoid phytoalexins in the leaves of SL mutants. The SL biosynthetic mutant *d10* and

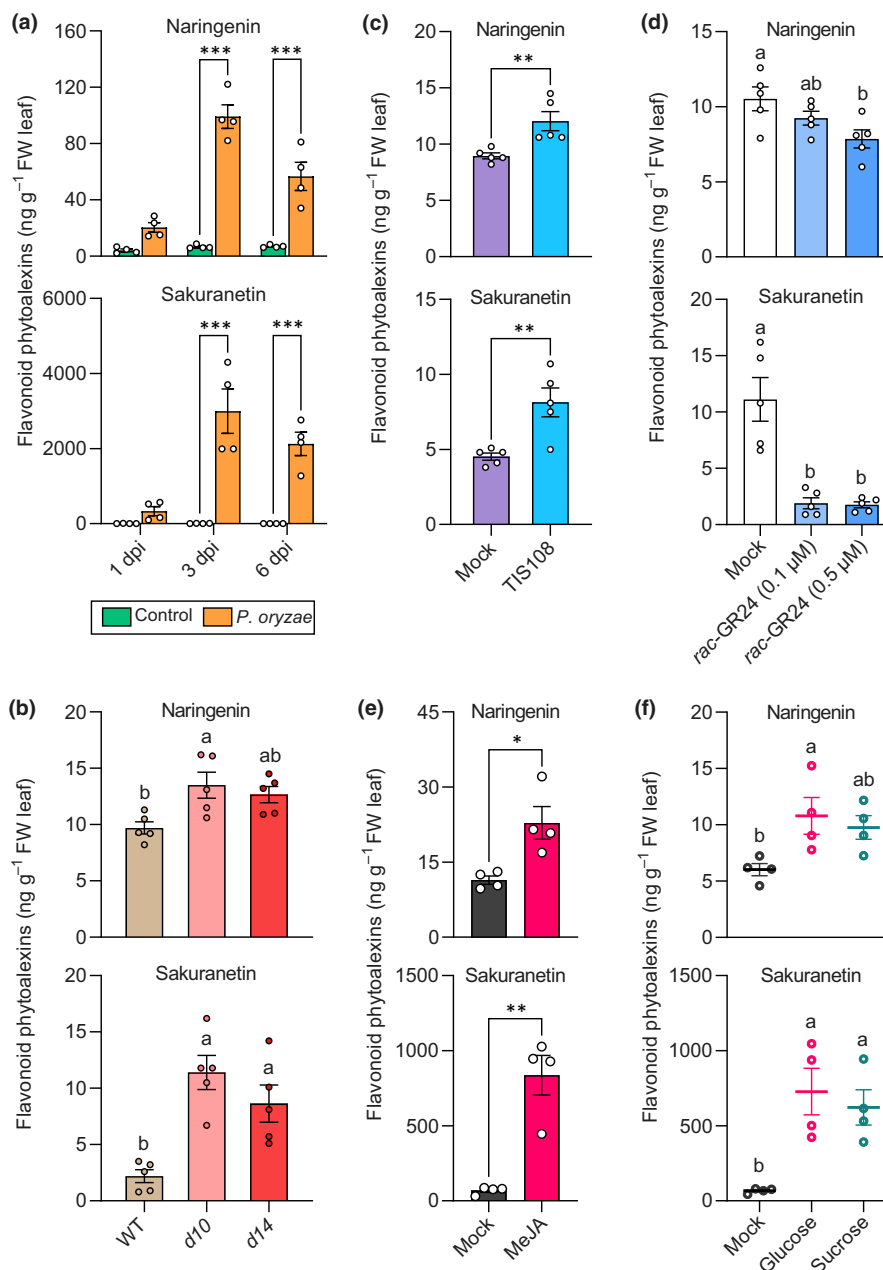


**Fig. 6** Strigolactones (SLs) negatively regulate the accumulation of flavonoid phytoalexins in rice leaves. (a) Naringenin and sakuranetin levels were induced in rice leaves in response to infection by the blast fungus *Pyricularia oryzae*. Leaf samples from fungus-infected and control plants were harvested at 1, 3 and 6 d post inoculation (dpi) in four biological replicates, each consisting of a pool of four-to-five seedlings grown in separate pots. Flavonoid levels were determined using a triple quadrupole mass spectrometer, and data were analyzed using a two-way ANOVA, followed by Tukey's multiple comparison test with a 95% confidence interval. Significantly different comparisons between control vs infected levels at each time point are displayed on graphs using asterisks (\*\*\*,  $P < 0.001$ ). Statistical details of a two-way ANOVA for the levels of flavonoid metabolites are provided in Supporting Information Table S11. Data are presented as the mean  $\pm$  SE, and all data points are shown on the graph as open circles ( $n = 4$ ). (b) The accumulation of flavonoid phytoalexins increased in SL biosynthetic (*d10*) and SL signaling (*d14*) mutants. Shoots of transplanted 2-wk-old rice seedlings were harvested in five biological replicates, each consisting of a pool of three-to-four seedlings grown in separate pots. Data were analyzed using a one-way ANOVA, followed by Tukey's test with a 95% confidence interval. Different letters above bars indicate groups that are significantly different ( $P < 0.05$ ). (c) Wild-type rice seedlings treated with the SL biosynthesis inhibitor TIS108 induced the accumulation of flavonoid phytoalexins. Shoots of TIS108-treated rice seedlings were harvested in five biological replicates, each consisting of a pool of three-to-four seedlings grown in separate pots. Flavonoid data were analyzed using a two-tailed *t*-test (\*\*,  $P < 0.01$ ). (d) Levels of flavonoid phytoalexins were reduced in rice seedlings treated with the SL analogue *rac*-GR24. Shoots of GR24-treated rice seedlings were harvested in five biological replicates, each consisting of a pool of three-to-four seedlings grown in separate pots. Flavonoid data were analyzed using a one-way ANOVA, followed by Tukey's test with a 95% confidence interval. Different letters above bars indicate groups that are significantly different ( $P < 0.05$ ). Data (b–e) are presented as the mean  $\pm$  SE, and all data points are shown on the graph as open circles ( $n = 4–5$ ). (e, f) Accumulation of flavonoid phytoalexins increased in the leaves of rice seedlings treated with MeJA and soluble sugars. Shoots of MeJA- and sugar-treated rice seedlings were harvested 1 d after respective chemical treatment in four biological replicates ( $n = 4$ ), each consisting of a pool of four to six seedlings. MeJA-treated data were analyzed using a two-tailed *t*-test (\*,  $P < 0.05$ ; \*\*,  $P < 0.01$ ). Sugar-treated data were analyzed using a one-way ANOVA, followed by Tukey's test with a 95% confidence interval. Different letters above bars (e) indicate groups that are significantly different ( $P < 0.05$ ). Data (f) are presented as scatter plots shown by the open circles, and solid lines represent mean  $\pm$  SE ( $n = 4$ ). All data points are shown on the graph as circles.

the signaling mutant *d14* both accumulated increased levels of naringenin and sakuranetin compared to the WT (Fig. 6b). Similarly, when WT seedlings were treated with the SL biosynthesis inhibitor TIS108, flavonoid phytoalexins accumulated in higher amounts than in untreated control seedlings (Fig. 6c). By contrast, WT seedlings treated with the SL analog *rac*-GR24 showed reduced levels of naringenin and sakuranetin (Fig. 6d). Since SL-deficient plants increased the levels of both jasmonates and soluble sugars, we quantified the concentrations of flavonoid phytoalexins after treatment with MeJA and soluble sugars. Both JA and sugar treatment significantly enhanced the accumulation of naringenin and sakuranetin (Fig. 6e,f). Collectively, these results suggest that SLs negatively regulate flavonoid phytoalexins, while jasmonate and soluble sugars increase flavonoid accumulation in rice leaves.

### Jasmonate and sugar signaling pathways interact positively in rice

It is now evident that jasmonates and sugars both induce flavonoid phytoalexins in rice. Concomitant accumulation of higher levels of sugars and jasmonates in SL-deficient rice seedlings as well as in WT plants after *P. oryzae* infection raised the question of whether JA signaling is directly connected to sugar accumulation and vice versa. To address this question, we quantified sugar accumulation in the *jar1* mutant and the *coi1-18* RNAi line. *jar1* encodes JAR1, an ATP-dependent JA-amido synthetase, which catalyzes the conjugation of isoleucine to JA, resulting in the formation of JA-Ile (Riemann *et al.*, 2008). JA-Ile is considered the most active JA metabolite perceived by the COI1 receptor, resulting in downstream JA signaling (Riemann *et al.*, 2008), while *coi1-18* is defective in JA response (Yang *et al.*, 2012). Concentrations of glucose and fructose were significantly lower in *jar1* and *coi1-18* lines than in the WT Nipponbare (Fig. 7a). However, the levels of sucrose and raffinose did not change in these lines (Fig. 7a). We also measured JA metabolites in these lines. Levels of *cis*-OPDA and JA

were similar in mutant and WT leaves (Fig. S8). JA-Ile and OH-JA-Ile concentrations were extremely low in the *jar1* mutant in comparison with both WT and *coi1-18* RNAi plants, which both accumulated comparable amounts of JA-Ile (Fig. S8). In a separate experiment, we compared sugar concentrations in WT seedlings (cv Shiokari) with and without MeJA treatment. After 24 h, the exogenous MeJA was readily converted to different forms of JA metabolites, including JA and JA-Ile (Fig. S9). Increased JA metabolites also enhanced total soluble sugar content, which is dominated by sucrose (Fig. S10), indicating a positive role of JA signaling in sugar accumulation.

To determine whether soluble sugars affect jasmonate accumulation, we treated 2-wk-old WT rice seedlings (cv Nipponbare) separately using glucose and sucrose. Leaf samples were collected after 24 h, and JA metabolites were analyzed using LC-MS/MS. Application of glucose or sucrose significantly induced the accumulation of the jasmonates measured (*cis*-OPDA, JA, JA-Ile, and OH-JA-Ile) in most cases, except for sucrose with *cis*-OPDA and JA (Fig. 7b). Levels of JA-Ile and OH-JA-Ile increased substantially after treatment with both glucose and sucrose in comparison with control seedlings (Fig. 7b). These findings suggest that sugar and jasmonate signaling pathways interact positively in rice.

### The antagonism between SL and jasmonate signaling mediates rice defense against *P. oryzae*

Since *rac*-GR24 application decreased JA-Ile content in WT and the SL biosynthetic mutant *d10*, but not the signaling mutant *d14* (Fig. S4), we carried out an infection experiment using the SL mutants and the corresponding WT (cv Shiokari) after complementing with *rac*-GR24. Seedlings of each line were treated with *rac*-GR24 or solvent only (mock) 24 h before *P. oryzae* inoculation. We found that pretreatment with *rac*-GR24 enhanced blast infection on WT and *d10* seedlings, as shown by quantifying sporulating lesion formation (Fig. 8a). However, the SL signaling mutant *d14* was insensitive to *rac*-

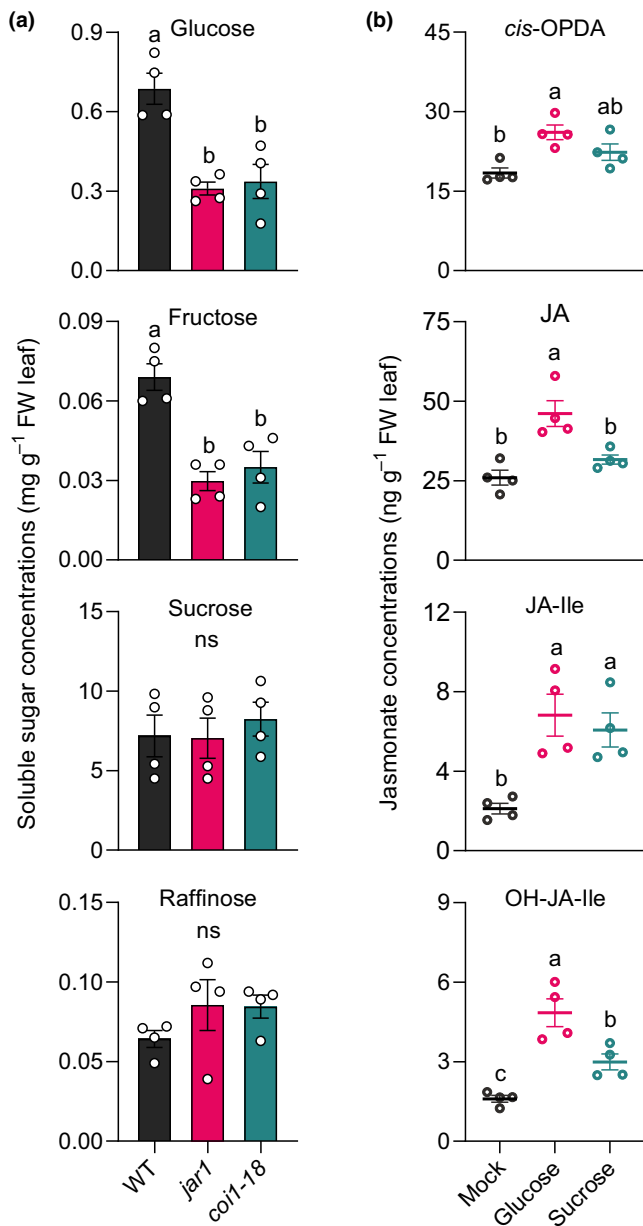


**Fig. 7** Positive interplay between sugars and jasmonate signaling in rice. (a) Concentrations of soluble sugars in rice mutants defective in jasmonoyl-L-isoleucine (JA-Ile) synthesis (*jar1*) and JA perception (*coi1-18*) compared with the wild-type Nipponbare. Leaf samples were harvested from 3-wk-old rice seedlings, and sugars were quantified using a triple quadrupole mass spectrometer. Data were analyzed using a one-way ANOVA, followed by Tukey's multiple comparison test with a 95% confidence interval. Different letters above bars indicate groups that are significantly different ( $P < 0.05$ ). Data are presented using bar plots as the mean  $\pm$  SE, and all data points are shown on the graph as open circles ( $n = 4$ ). (b) Accumulation of jasmonates in rice leaves after treatment with sugars. Three-week-old rice seedlings were sprayed with glucose, sucrose or with solvent only as a mock control. Leaf samples were harvested 24 h after treatment. Data are presented as scatter plots shown by the open circles, and solid lines represent mean  $\pm$  SE ( $n = 4$ ). Hormone data were analyzed using a one-way ANOVA, followed by Tukey's multiple comparison test with a 95% confidence interval. Different letters above scattered plots indicate groups that are significantly different ( $P < 0.05$ ). All data points are plotted as open circles ( $n = 4$ ). *cis*-OPDA, *cis*-(+)-12-oxo-phytodienoic acid; OH-JA-Ile, 12-hydroxy-JA-Ile; JA, jasmonic acid; JA-Ile, jasmonoyl-isoleucine; ns, nonsignificant.

GR24, resulting in similar infection levels observed in the untreated *dl4* plants (Fig. 8a,b). Next, we conducted another infection assay using the *jar1* mutant, defective in JA-Ile accumulation, the *coi1-18* RNAi line, defective in jasmonate perception and the corresponding WT (cv Nipponbare). Half of the seedlings of each line were also sprayed with the SL inhibitor TIS108 24 h before *P. oryzae* inoculation. The WT seedlings pretreated with TIS108 displayed enhanced resistance against *P. oryzae* (Fig. 8c). The *jar1* mutant showed a higher number of susceptible lesions than the WT plants, suggesting that JA-Ile production is necessary for blast resistance in rice. Furthermore, the JA signaling-deficient *coi1-18* RNAi line was hypersensitive to *P. oryzae* infection, with three times higher numbers of sporulating lesions than the WT (Fig. 8c). However, pretreatment with TIS108 did not reduce the susceptibility of *jar1* and *coi1-18* mutants (Fig. 8c,d), suggesting that rice defense against *P. oryzae* caused by attenuated SL signaling is dependent on JA-Ile production and intact JA signaling.

## Discussion

The carotenoid-derived SLs are well-known for their functions in plant growth and development (Gomez-Roldan *et al.*, 2008; Umehara *et al.*, 2008; Sun *et al.*, 2014; Ueda & Kusaba, 2015; Ravazzolo *et al.*, 2021). However, the role of these hormones in plant defense against pathogens, especially those causing foliar diseases, is less understood. Here, we provide decisive evidence that inhibition of SL biosynthesis and signaling enhances rice defense against the leaf blast fungus *P. oryzae* through a higher accumulation of soluble sugars, jasmonates and flavonoid phytoalexins such as naringenin and sakuranetin. We also report a reciprocal positive interplay between JA signaling and soluble sugar concentrations in rice leaves.

### The reciprocal positive interplay between soluble sugars and jasmonates in rice

Soluble sugars, such as glucose, fructose, sucrose and raffinose, are more than just energy sources in plants but are involved in integrating environmental cues via osmotic adjustments, ROS homeostasis and effects on hormones (Kanwar & Jha, 2019; Saddhe *et al.*, 2021). Auxin, cytokinin, salicylic acid, abscisic acid and ethylene signaling pathways are modulated by sugar-sensing proteins such as hexokinases and sucrose transporters (Choudhary *et al.*, 2022). In the JA pathway, sugars regulate key signaling genes such as *MYC2*. The current study showed that foliar treatments with glucose or sucrose in rice enhance jasmonate accumulation in leaves, indicating positive crosstalk between sugar and JA signaling pathways. Reciprocally, we found a significant increase in total soluble sugar content, predominantly sucrose, in rice seedlings after MeJA treatment (Fig. S10). These findings are supported by a recent study on ryegrass in which MeJA markedly induced the *LpSUCT1* gene and increased sucrose content in leaves (Meuriot *et al.*, 2022). Exogenous MeJA is readily converted to various jasmonates, including the most active jasmonate JA-Ile, thereby triggering the JA signaling pathway. However, the

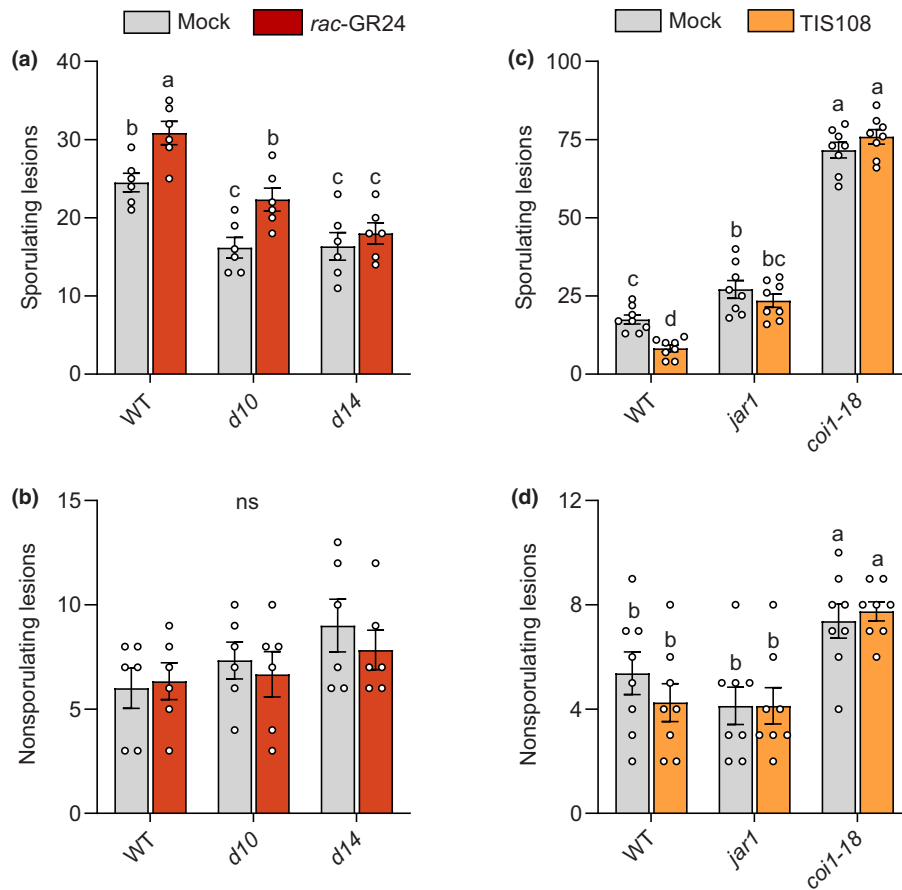


**Fig. 8** Complementation experiments using the strigolactone (SL) analogue *rac*-GR24 and the SL biosynthetic inhibitor TIS108. (a, b) Pretreatment with *rac*-GR24 increases rice susceptibility to *Pyricularia oryzae* in wild-type (WT) and SL biosynthetic mutant *d10* but does not affect the signaling mutant *d14*. Two-week-old transplanted rice seedlings of all lines were treated with *rac*-GR24 or with the mock control. (c, d) The SL biosynthetic inhibitor TIS108 reduces *P. oryzae* infection in WT (cv Nipponbare) but not in *jar1* mutant and *coi1-18* RNAi lines. The mutant *jar1* is defective in jasmonoyl-L-isoleucine (JA-Ile) biosynthesis, and the *coi1-18* RNAi line has reduced jasmonate perception. Two-week-old transplanted rice seedlings of all lines were treated with TIS108 or with the mock control. In both experiments, 1 d after chemical treatments, all seedlings were inoculated with the blast fungus *P. oryzae*, and the disease was scored 6 d post inoculation (dpi). Infection levels were determined by counting the average number of sporulating (a, c) and nonsporulating (b, d) lesions on the second youngest leaf. Data were analyzed using a two-way ANOVA, followed by Tukey's multiple comparisons test with a 95% confidence interval. Statistical details of a two-way ANOVA are provided in Supporting Information Tables S12 and S13. Different letters above bars indicate significantly different groups ( $P < 0.05$ ). Data are presented as the mean  $\pm$  SE, and all data points are shown on the graph as open circles ( $n = 6-8$ ). ns, nonsignificant.

*jar1* mutant, which cannot synthesize JA-Ile (Riemann *et al.*, 2008), and *coi1-18* silenced plants, which are perturbed in jasmonate perception (Yang *et al.*, 2012), both accumulated lower levels of soluble sugars, mainly glucose and fructose (Fig. 7a). The lack of a significant decline in sucrose may arise from the faster growth of the JA mutants, which may be correlated with a higher photosynthetic rate and thus higher sucrose levels. Our results indicate a mutual positive interplay between sugar and JA signaling pathways in rice, which may provide fitness benefits under changing environmental conditions.

### SLs antagonize the accumulation of soluble sugars, jasmonates and flavonoid phytoalexins

Soluble sugars are known to suppress the function of SLs in different plant species. For example, glucose inhibited SL-induced leaf senescence in bamboo and rice (Tian *et al.*, 2018; Takahashi *et al.*, 2021). Likewise, sucrose was found to suppress SL-mediated

inhibition of axillary bud outgrowth in rose and pea (Bertheloot *et al.*, 2020) and tillering in rice (Patil *et al.*, 2022). In the current study, we asked whether SLs modulate soluble sugar content in rice using three different approaches: after exogenous application of a synthetic SL, *rac*-GR24; after spraying with the SL inhibitor TIS108; and using rice mutants perturbed in SL biosynthesis (*d10*) and signaling (*d14*). Treatment with *rac*-GR24 reduced sugar concentrations in rice leaves, while the inhibitor TIS108 increased the levels of sucrose and raffinose compared to those in mock-treated plants. Finally, enhanced sugar concentrations were found in rice mutants compared with WT plants. These results establish that SL signaling negatively affects sugar content in rice shoots. However, *Arabidopsis* lines overexpressing *MAX2*, a central component of the SL signaling cascade, accumulated higher soluble sugar content compared with WT in response to drought and salinity stresses (Wang *et al.*, 2019). Moreover, *max1* and *max2* mutants accumulated slightly lower levels of hexose sugars without affecting sucrose and starch content (Li *et al.*, 2016). It appears

that the outcome of SL-mediated sugar signaling is different in rice and *Arabidopsis*.

Recent studies have revealed that SLs antagonize the JA signaling pathway in the roots of rice (Lahari *et al.*, 2019) and tomato (Xu *et al.*, 2019), and the stems of *Nicotiana attenuata* (Li *et al.*, 2020). Given that soluble sugars and JA metabolites induce each other, we anticipated that rice seedlings blocked in SL signaling would display higher levels of jasmonates, and this was confirmed for the *d10* and *d14* mutants and in plants sprayed with the SL biosynthetic inhibitor TIS108 (Fig. 2). Application of the SL analogue *rac*-GR24 decreased jasmonate content, especially JA-Ile. The negative effect of SLs on jasmonates was further supported by the restoration of basal jasmonate levels in the leaves of SL biosynthetic mutant *d10* by *rac*-GR24 treatment (Fig. S4). Previously, it was shown that *rac*-GR24 also restored the susceptibility of root-knot nematode infection in SL-deficient lines, while the SL perception mutant *d14* was unaffected (Lahari *et al.*, 2019). However, further investigation is necessary to determine how SL mutants and WT seedlings respond to specific stereoisomers of GR24, as plants respond slightly differently to GR24<sup>5DS</sup> and GR24<sup>ent-5DS</sup> (Zheng *et al.*, 2020).

Upon pathogen attack, flavonoids are often highly induced in plants resulting in increased disease resistance (Liu *et al.*, 2010; Miyamoto *et al.*, 2016; Ullah *et al.*, 2017; Förster *et al.*, 2022). As reported earlier and in the current study, levels of the flavanone flavonoids naringenin and sakuranetin increased remarkably in rice leaves in response to *P. oryzae* infection. Our study also revealed a novel negative link between SLs and these phytoalexins. Besides the simultaneous accumulation of jasmonates and soluble sugars, SL-deficient plants constitutively increased their levels of naringenin and sakuranetin. In separate experiments, we also found that jasmonates and sugars increased naringenin and sakuranetin levels in rice leaves (Fig. 6). In grapes, GR24 was shown to inhibit the accumulation of anthocyanin (Ferrero *et al.*, 2018). We also found a similar effect of *rac*-GR24 on rice flavonoid phytoalexins. By contrast, several genes involved in flavonoid biosynthesis were downregulated in the arabidopsis *max1* mutant (Lazar & Goodman, 2006), indicating that SLs might regulate certain classes of flavonoids in different ways in different plant species. Further studies are necessary to unravel how SL signaling is linked to phytoalexin accumulation in other plants.

### SL deficiency enhances rice defense against *P. oryzae* via jasmonates and sugars

The two most evolutionary conserved functions of SLs in plant biotic interactions are to facilitate symbiosis with beneficial microbes and trigger the germination of parasitic weed seeds. While the former is a positive trait for plant survival, the latter is a negative trait, at least for the host of the parasite. Strigolactones also play disparate roles in plant defense against different pathogens, which could be due to various factors such as the plant species, developmental stage, tissue specificity and the pathogen lifestyle (Dor *et al.*, 2011; Torres-Vera *et al.*, 2014; Lahari *et al.*, 2019; Xu *et al.*, 2019). In rice roots, SLs promote infection by the root-knot nematode *Meloidogyne graminicola* (Lahari *et al.*, 2019). This obligate biotrophic pathogen

manipulates root cell metabolism extensively and suppresses plant defense during parasitism (Mantelin *et al.*, 2017; Lahari *et al.*, 2019). One of the central research questions of the current study was to determine the role of SLs in rice shoots against the hemibiotrophic fungus *P. oryzae*, which causes blast disease at all stages of rice growth and is considered to be one of the most destructive fungal plant pathogens in the world (Dean *et al.*, 2012). Infection experiments using a virulent strain (VT5M1) on seedlings of both SL biosynthetic and signaling mutants (*d10* and *d14*, respectively), clearly showed that SL mutants were less susceptible than the corresponding WT Shiokari. Furthermore, WT seedlings that were pretreated with the SL analog *rac*-GR24 enhanced *P. oryzae* susceptibility. Blast susceptibility was also restored in the SL biosynthetic mutant *d10* when *rac*-GR24 was applied before fungal inoculation. However, the SL signaling mutant *d14* was not responsive to *rac*-GR24. By contrast, another study demonstrated that rice *d17* and *d14* mutants were more susceptible than WT to *P. oryzae* (Nasir *et al.*, 2019). However, in this study, the WT plants appeared almost immune to the fungal strain used for the infection experiment. To confirm our observations, WT rice seedlings were pretreated with the SL biosynthesis inhibitor TIS108 and subsequently infected by the fungus. Here, we also observed reduced blast susceptibility in SL-deficient rice seedlings.

In the same way that SLs influence resistance to *P. oryzae* infection in rice leaves, this hemibiotrophic fungus influenced SL abundance over the time course of this compatible plant–pathogen interaction. For example, we showed that SL biosynthetic and signaling genes were downregulated in *P. oryzae*-infected tissues accompanied by an increase in the levels of soluble sugars and jasmonates compared with the control. As discussed above, induced sugars might be involved in defense signaling. For

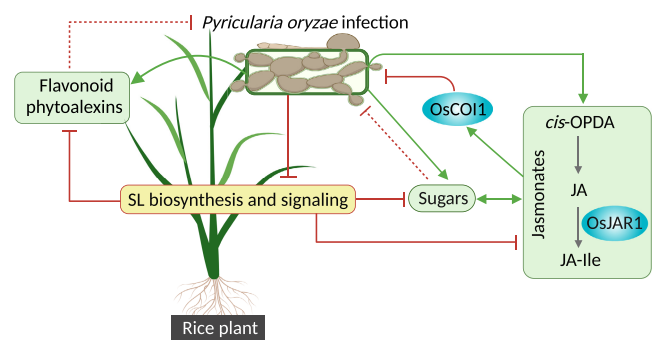


**Fig. 9** Schematic model depicts how strigolactones (SLs) suppress rice defense against *Pyricularia oryzae* by inhibiting jasmonate, sugar and flavonoid phytoalexin accumulation. *Pyricularia oryzae* infection in rice leaves, as well as the chemical treatment and genetic mutants used here, result in the downregulation of SL biosynthesis and signaling, which markedly increases the accumulation of soluble sugars, jasmonates and flavonoid phytoalexins including naringenin and sakuranetin. These known antifungal flavonoids are also induced by both jasmonate and sugar treatments. Activation of the jasmonate pathway increases defense against the blast fungus. Green lines with arrowheads depict positive relationships, and red lines with blunt ends represent inhibition or negative relationships. The dashed line indicates a relationship supported by the literature. *cis*-OPDA, *cis*-(+)-12-oxo-phytodienoic acid; JA, jasmonic acid; JA-Ile, jasmonyl-isoleucine.

example, rice plants overexpressing the pathogenesis-related gene *PRms* had higher sucrose accumulation and increased resistance against *P. oryzae* (Gómez-Ariza *et al.*, 2007). Exogenous sugar application was also shown to reduce *P. oryzae* infection. In rice, jasmonates are considered to be the major hormone triggering antipathogen defenses, and JA biosynthesis and signaling genes were induced in rice leaves infected by *P. oryzae* (Zhang *et al.*, 2018). While infection experiments with virulent *P. oryzae* strains on several rice lines deficient in JA biosynthesis (e.g. *aoc-RNAi*, *opr7-RNAi* and *aoc*) did not show greater *P. oryzae* infectivity than on control rice lines (Yara *et al.*, 2008; Riemann *et al.*, 2013), exogenous treatments with MeJA (Zhang *et al.*, 2018) and JA (Wang *et al.*, 2021) strongly reduced *P. oryzae* infection. Our study has substantiated the role of JA signaling and the bioactive JA-Ile in rice defense against the blast pathogen. The *jar1* mutant and *coi1-18* RNAi lines were more susceptible to *P. oryzae* than WT. Moreover, since SL deficiency was found to increase jasmonate accumulation, we treated WT rice seedlings with the SL inhibitor TIS108. This treatment not only increased the levels of JA and other jasmonates, but also reduced blast infection in WT plants, affirming that rice defense against the blast fungus is dependent on JA signaling.

## Conclusion

Our results show that rice seedlings respond to *P. oryzae* infection by downregulating the SL signaling pathway, which results in increased accumulation of soluble sugars, jasmonates and flavonoid phytoalexins. Loss-of-function SL mutants also displayed increased soluble sugar and jasmonate levels, and greater amounts of antimicrobial flavonoids resulting in increased resistance to the blast fungus. Transgenic rice lines with attenuated JA-Ile production or reduced JA signaling were more susceptible to the fungus, but this could not be changed by inhibiting the SL pathway. We propose that rice SL-deficiency-mediated defense against the blast fungus *P. oryzae* functions via the JA signaling pathway, and that it is also strongly linked to sugar signaling pathways (Fig. 9).

## Acknowledgements

We thank Prof. Mikio Nakazono, Nagoya University, and Dr Itsuro Takamura, Hokkaido University, Japan, for providing seeds of SL mutants. This work was jointly financed by the Special Research Fund of Ghent University via the BOF13/GOA/030 project, and Max Planck Society. Open Access funding enabled and organized by Projekt DEAL.

## Competing interests



None declared.

## Author contributions

CU, ZL and GG conceived this study. CU, ZL, GG, JG and MH designed experiments and interpreted the results. ZL, CU,

SVB and OOO conducted all experiments. MR contributed to the development of analytical methods. CU and GG supervised the project. CU prepared figures, analyzed data and wrote the manuscript with input from ZL. All authors read, provided comments and approved the final version of the manuscript.

## ORCID

Sarah van Boerdonk  <https://orcid.org/0000-0003-2671-344X>  
Jonathan Gershenzon  <https://orcid.org/0000-0002-1812-1551>

Godelieve Gheysen  <https://orcid.org/0000-0003-1929-5059>

Monica Höfte  <https://orcid.org/0000-0002-0850-3249>

Zobaida Lahari  <https://orcid.org/0000-0003-4765-7547>

Olumide Owolabi Omoboye  <https://orcid.org/0000-0002-6403-9567>

Michael Reichelt  <https://orcid.org/0000-0002-6691-6500>

Chhana Ullah  <https://orcid.org/0000-0002-8898-669X>

## Data availability

All data supporting the findings of this work are available within the paper and [Supporting Information](#).

## References

- Akiyama K, Matsuzaki K-i, Hayashi H. 2005. Plant sesquiterpenes induce hyphal branching in arbuscular mycorrhizal fungi. *Nature* 435: 824–827.
- Alder A, Jamil M, Marzorati M, Bruno M, Vermathen M, Bigler P, Ghisla S, Bouwmeester H, Beyer P, Al-Babili S. 2012. The path from  $\beta$ -carotene to carlactone, a strigolactone-like plant hormone. *Science* 335: 1348–1351.
- Barbier FF, Lunn JE, Beveridge CA. 2015. Ready, steady, go! A sugar hit starts the race to shoot branching. *Current Opinion in Plant Biology* 25: 39–45.
- Bertheloot J, Barbier F, Boudon F, Perez-Garcia MD, Péron T, Citerne S, Dun E, Beveridge C, Godin C, Sakr S. 2020. Sugar availability suppresses the auxin-induced strigolactone pathway to promote bud outgrowth. *New Phytologist* 225: 866–879.
- Blake SN, Barry KM, Gill WM, Reid JB, Foo E. 2016. The role of strigolactones and ethylene in disease caused by *Pythium irregulare*. *Molecular Plant Pathology* 17: 680–690.
- Bu Q, Lv T, Shen H, Luong P, Wang J, Wang Z, Huang Z, Xiao L, Engineer C, Kim TH. 2014. Regulation of drought tolerance by the F-box protein MAX2 in *Arabidopsis*. *Plant Physiology* 164: 424–439.
- Chakraborty S, Hill AL, Shirsekar G, Afzal AJ, Wang G-L, Mackey D, Bonello P. 2016. Quantification of hydrogen peroxide in plant tissues using Amplex Red. *Methods* 109: 105–113.
- Choudhary A, Kumar A, Kaur N, Kaur H. 2022. Molecular cues of sugar signaling in plants. *Physiologia Plantarum* 174: e13630.
- Cook C, Whichard LP, Turner B, Wall ME, Egley GH. 1966. Germination of witchweed (*Striga lutea* Lour.): isolation and properties of a potent stimulant. *Science* 154: 1189–1190.
- Das D, Paries M, Hobecker K, Gigl M, Dawid C, Lam H-M, Zhang J, Chen M, Gutjahr C. 2022. PHOSPHATE STARVATION RESPONSE transcription factors enable arbuscular mycorrhiza symbiosis. *Nature Communications* 13: 1–12.
- De Vleeschauwer D, Cornelis P, Höfte M. 2006. Redox-active pyocyanin secreted by *Pseudomonas aeruginosa* 7NSK2 triggers systemic resistance to *Magnaporthe grisea* but enhances *Rhizoctonia solani* susceptibility in rice. *Molecular Plant–Microbe Interactions* 19: 1406–1419.
- Dean R, Van Kan JA, Pretorius ZA, Hammond-Kosack KE, Di Pietro A, Spanu PD, Rudd JJ, Dickman M, Kahmann R, Ellis J. 2012. The Top 10 fungal

- pathogens in molecular plant pathology. *Molecular Plant Pathology* 13: 414–430.
- Decker EL, Alder A, Hunn S, Ferguson J, Lehtonen MT, Scheler B, Kerres KL, Wiedemann G, Safavi-Rizi V, Nordziske S. 2017. Strigolactone biosynthesis is evolutionarily conserved, regulated by phosphate starvation and contributes to resistance against phytopathogenic fungi in a moss, *Physcomitrella patens*. *New Phytologist* 216: 455–468.
- Dor E, Joel DM, Kapulnik Y, Koltai H, Hershenhorn J. 2011. The synthetic strigolactone GR24 influences the growth pattern of phytopathogenic fungi. *Planta* 234: 419.
- Escudero Martinez CM, Guarneri N, Overmars H, van Schaik C, Bouwmeester H, Ruyter-Spira C, Goverse A. 2019. Distinct roles for strigolactones in cyst nematode parasitism of *Arabidopsis* roots. *European Journal of Plant Pathology* 154: 129–140.
- Ferrero M, Pagliarini C, Novák O, Ferrandino A, Cardinale F, Visentin I, Schubert A. 2018. Exogenous strigolactone interacts with abscisic acid-mediated accumulation of anthocyanins in grapevine berries. *Journal of Experimental Botany* 69: 2391–2401.
- Fonseca S, Chini A, Hamberg M, Adie B, Porzel A, Kramell R, Miersch O, Wasternack C, Solano R. 2009. (+)-7-iso-Jasmonoyl-L-isoleucine is the endogenous bioactive jasmonate. *Nature Chemical Biology* 5: 344–350.
- Förster C, Handrick V, Ding Y, Nakamura Y, Paetz C, Schneider B, Castro-Falcón G, Hughes CC, Luck K, Poosapati S *et al.* 2022. Biosynthesis and antifungal activity of fungus-induced O-methylated flavonoids in maize. *Plant Physiology* 188: 167–190.
- Gómez-Ariza J, Campo S, Rufat M, Estopà M, Messegue J, Segundo BS, Coca M. 2007. Sucrose-mediated priming of plant defense responses and broad-spectrum disease resistance by overexpression of the maize pathogenesis-related PRms protein in rice plants. *Molecular Plant–Microbe Interactions* 20: 832–842.
- Gomez-Roldan V, Fervas S, Brewer PB, Puech-Pagès V, Dun EA, Pillot J-P, Letisse F, Matusova R, Danoun S, Portais J-C. 2008. Strigolactone inhibition of shoot branching. *Nature* 455: 189–194.
- Guo Q, Major IT, Howe GA. 2018. Resolution of growth–defense conflict: mechanistic insights from jasmonate signaling. *Current Opinion in Plant Biology* 44: 72–81.
- Ha CV, Leyva-González MA, Osakabe Y, Tran UT, Nishiyama R, Watanabe Y, Tanaka M, Seki M, Yamaguchi S, Dong NV. 2014. Positive regulatory role of strigolactone in plant responses to drought and salt stress. *Proceedings of the National Academy of Sciences, USA* 111: 851–856.
- Ito S, Umehara M, Hanada A, Kitahata N, Hayase H, Yamaguchi S, Asami T. 2011. Effects of triazole derivatives on strigolactone levels and growth retardation in rice. *PLoS ONE* 6: e21723.
- Kalliola M, Jakobson L, Davidsson P, Pennanen V, Waszczak C, Yarmolinsky D, Zamora O, Palva ET, Kariola T, Kollist H. 2020. Differential role of MAX2 and strigolactones in pathogen, ozone, and stomatal responses. *Plant Direct* 4: e00206.
- Kameoka H, Kyozuka J. 2018. Spatial regulation of strigolactone function. *Journal of Experimental Botany* 69: 2255–2264.
- Kanwar P, Jha G. 2019. Alterations in plant sugar metabolism: signatory of pathogen attack. *Planta* 249: 305–318.
- Kou Y, Qiu J, Tao Z. 2019. Every coin has two sides: reactive oxygen species during Rice–*Magnaporthe oryzae* interaction. *International Journal of Molecular Sciences* 20: 1191.
- Kumar M, Pandya-Kumar N, Kapulnik Y, Koltai H. 2015. Strigolactone signaling in root development and phosphate starvation. *Plant Signaling & Behavior* 10: e1045174.
- Lahari Z, Ullah C, Kyndt T, Gershenzon J, Gheysen G. 2019. Strigolactones enhance root-knot nematode (*Meloidogyne graminicola*) infection in rice by antagonizing the jasmonate pathway. *New Phytologist* 224: 454–465.
- Lazar G, Goodman HM. 2006. MAX1, a regulator of the flavonoid pathway, controls vegetative axillary bud outgrowth in *Arabidopsis*. *Proceedings of the National Academy of Sciences, USA* 103: 472–476.
- Li GD, Pan LN, Jiang K, Takahashi I, Nakamura H, Xu YW, Asami T, Shen RF. 2016. Strigolactones are involved in sugar signaling to modulate early seedling development in *Arabidopsis*. *Plant Biotechnology* 33: 87–97.
- Li S, Joo Y, Cao D, Li R, Lee G, Halitschke R, Baldwin G, Baldwin IT, Wang M. 2020. Strigolactone signaling regulates specialized metabolism in tobacco stems and interactions with stem-feeding herbivores. *PLoS Biology* 18: e3000830.
- Liu H, Du Y, Chu H, Shih CH, Wong YW, Wang M, Chu IK, Tao Y, Lo C. 2010. Molecular dissection of the pathogen-inducible 3-deoxyanthocyanidin biosynthesis pathway in *Sorghum*. *Plant and Cell Physiology* 51: 1173–1185.
- López-Ráez JA, Shirasu K, Foo E. 2017. Strigolactones in plant interactions with beneficial and detrimental organisms: the Yin and Yang. *Trends in Plant Science* 22: 527–537.
- Ma N, Hu C, Wan L, Hu Q, Xiong J, Zhang C. 2017a. Strigolactones improve plant growth, photosynthesis, and alleviate oxidative stress under salinity in rapeseed (*Brassica napus* L.) by regulating gene expression. *Front. Plant Science* 8: 1671.
- Ma Z, Ongena M, Höfte M. 2017b. The cyclic lipopeptide orfamide induces systemic resistance in rice to *Cochliobolus miyabeanus* but not to *Magnaporthe oryzae*. *Plant Cell Reports* 36: 1731–1746.
- Machin DC, Hamon-Josse M, Bennett T. 2020. Fellowship of the rings: a saga of strigolactones and other small signals. *New Phytologist* 225: 621–636.
- Mantelin S, Bellafiore S, Kyndt T. 2017. *Meloidogyne graminicola*: a major threat to rice agriculture. *Molecular Plant Pathology* 18: 3.
- Mashiguchi K, Seto Y, Yamaguchi S. 2021. Strigolactone biosynthesis, transport and perception. *The Plant Journal* 105: 335–350.
- Meuriot F, Prud'homme MP, Noiraud-Romy N. 2022. Defoliation, wounding, and methyl jasmonate induce expression of the sucrose lateral transporter LpSUT1 in ryegrass (*Lolium perenne* L.). *Physiologia Plantarum* 174: e13744.
- Miyamoto K, Enda I, Okada T, Sato Y, Watanabe K, Sakazawa T, Yumoto E, Shibata K, Asahina M, Iino M *et al.* 2016. Jasmonoyl-L-isoleucine is required for the production of a flavonoid phytoalexin but not diterpenoid phytoalexins in ultraviolet-irradiated rice leaves. *Bioscience, Biotechnology, and Biochemistry* 80: 1934–1938.
- Miyao A, Tanaka K, Murata K, Sawaki H, Takeda S, Abe K, Shinozuka Y, Onosato K, Hirochika H. 2003. Target site specificity of the Tos17 retrotransposon shows a preference for insertion within genes and against insertion in retrotransposon-rich regions of the genome. *Plant Cell* 15: 1771–1780.
- Monte I, Ishida S, Zamarreño AM, Hamberg M, Franco-Zorrilla JM, García-Casado G, Gouhier-Darimont C, Reymond P, Takahashi K, García-Mina JM. 2018. Ligand-receptor co-evolution shaped the jasmonate pathway in land plants. *Nature Chemical Biology* 14: 480–488.
- Nasir F, Tian L, Shi S, Chang C, Ma L, Gao Y, Tian C. 2019. Strigolactones positively regulate defense against *Magnaporthe oryzae* in rice (*Oryza sativa*). *Plant Physiology and Biochemistry* 142: 106–116.
- Ogawa S, Miyamoto K, Nemoto K, Sawasaki T, Yamane H, Nojiri H, Okada K. 2017. OsMYC2, an essential factor for JA-inductive sakuranetin production in rice, interacts with MYC2-like proteins that enhance its transactivation ability. *Scientific Reports* 7: 40175.
- Omoarelojie L, Kulkarni M, Finnie J, Van Staden J. 2019. Strigolactones and their crosstalk with other phytohormones. *Annals of Botany* 124: 749–767.
- Patil SB, Barbier FF, Zhao J, Zafar SA, Uzair M, Sun Y, Fang J, Perez-Garcia MD, Bertheloot J, Sakr S. 2022. Sucrose promotes D53 accumulation and tillering in rice. *New Phytologist* 234: 122–136.
- Pauwels L, Goossens A. 2011. The JAZ proteins: a crucial interface in the jasmonate signaling cascade. *Plant Cell* 23: 3089–3100.
- Piisilä M, Keceli MA, Brader G, Jakobson L, Joesar I, Sipari N, Kollist H, Palva ET, Kariola T. 2015. The F-box protein MAX2 contributes to resistance to bacterial phytopathogens in *Arabidopsis thaliana*. *BMC Plant Biology* 15: 1–17.
- Poudel AN, Holtsclaw RE, Kimberlin A, Sen S, Zeng S, Joshi T, Lei Z, Sumner LW, Singh K, Matsuura H. 2019. 12-Hydroxy-jasmonoyl-L-isoleucine is an active jasmonate that signals through CORONATINE INSENSITIVE 1 and contributes to the wound response in *Arabidopsis*. *Plant and Cell Physiology* 60: 2152–2166.
- Ravazzolo L, Boutet-Mercy S, Perreau F, Forestan C, Varotto S, Ruperti B, Quaggiotti S. 2021. Strigolactones and auxin cooperate to regulate maize root development and response to nitrate. *Plant and Cell Physiology* 62: 610–623.



- Riemann M, Haga K, Shimizu T, Okada K, Ando S, Mochizuki S, Nishizawa Y, Yamanouchi U, Nick P, Yano M. 2013. Identification of rice Allene Oxide Cyclase mutants and the function of jasmonate for defence against *Magnaporthe oryzae*. *The Plant Journal* 74: 226–238.
- Riemann M, Riemann M, Takano M. 2008. Rice JASMONATE RESISTANT 1 is involved in phytochrome and jasmonate signalling. *Plant, Cell & Environment* 31: 783–792.
- Ruan J, Zhou Y, Zhou M, Yan J, Khurshid M, Weng W, Cheng J, Zhang K. 2019. Jasmonic acid signaling pathway in plants. *International Journal of Molecular Sciences* 20: 2479.
- Saddhe AA, Manuka R, Penna S. 2021. Plant sugars: homeostasis and transport under abiotic stress in plants. *Physiologia Plantarum* 171: 739–755.
- Sattar A, Ul-Allah S, Ijaz M, Sher A, Butt M, Abbas T, Irfan M, Fatima T, Alfarraj S, Alharbi SA. 2022. Exogenous application of strigolactone alleviates drought stress in maize seedlings by regulating the physiological and antioxidants defense mechanisms. *Cereal Research Communications* 50: 263–272.
- Seto Y, Yasui R, Kameoka H, Tamiru M, Cao M, Terauchi R, Sakurada A, Hirano R, Kisugi T, Hanada A. 2019. Strigolactone perception and deactivation by a hydrolase receptor DWARF14. *Nature Communications* 10: 1–10.
- Steinkellner S, Lenzemo V, Langer I, Schweiger P, Khaosaad T, Toussaint J-P, Vierheilig H. 2007. Flavonoids and strigolactones in root exudates as signals in symbiotic and pathogenic plant–fungus interactions. *Molecules* 12: 1290–1306.
- Stes E, Dupuydt S, De Keyser A, Matthys C, Audenaert K, Yoneyama K, Werbrouck S, Goormachtig S, Vereecke D. 2015. Strigolactones as an auxiliary hormonal defence mechanism against leafy gall syndrome in *Arabidopsis thaliana*. *Journal of Experimental Botany* 66: 5123–5134.
- Sun H, Tao J, Liu S, Huang S, Chen S, Xie X, Yoneyama K, Zhang Y, Xu G. 2014. Strigolactones are involved in phosphate- and nitrate-deficiency-induced root development and auxin transport in rice. *Journal of Experimental Botany* 65: 6735–6746.
- Takahashi I, Jiang K, Asami T. 2021. Counteractive effects of sugar and strigolactone on leaf senescence of rice in darkness. *Agronomy* 11: 1044.
- Talbot NJ, Ebbolle DJ, Hamer JE. 1993. Identification and characterization of MPG1, a gene involved in pathogenicity from the rice blast fungus *Magnaporthe grisea*. *Plant Cell* 5: 1575–1590.
- Thuan NTN, Bigirimana J, Roumen E, Van Der Straeten D, Höfte M. 2006. Molecular and pathotype analysis of the rice blast fungus in North Vietnam. *European Journal of Plant Pathology* 114: 381–396.
- Tian M-q, Jiang K, Takahashi I, Li G-d. 2018. Strigolactone-induced senescence of a bamboo leaf in the dark is alleviated by exogenous sugar. *Journal of Pesticide Science* 43: 173–179.
- Torres-Vera R, García JM, Pozo MJ, López-Ráez JA. 2014. Do strigolactones contribute to plant defence? *Molecular Plant Pathology* 15: 211–216.
- Tun W, Yoon J, Vo KTX, Cho L-H, Hoang TV, Peng X, Kim E-J, Win KTYS, Lee S-W, Jung K-H *et al.* 2023. Sucrose preferentially promotes expression of *OsWRKY7* and *OsPRI0a* to enhance defense response to blast fungus in rice. *Frontiers in Plant Science* 14: 1117023.
- Ueda H, Kusaba M. 2015. Strigolactone regulates leaf senescence in concert with ethylene in *Arabidopsis*. *Plant Physiology* 169: 138–147.
- Ullah C, Schmidt A, Reichelt M, Tsai C-J, Gershenzon J. 2022. Lack of antagonism between salicylic acid and jasmonate signalling pathways in poplar. *New Phytologist* 235: 701–717.
- Ullah C, Unsicker SB, Fellenberg C, Constabel CP, Schmidt A, Gershenzon J, Hammerbacher A. 2017. Flavan-3-ols are an effective chemical defense against rust infection. *Plant Physiology* 175: 1560–1578.
- Umehara M, Hanada A, Yoshida S, Akiyama K, Arite T, Takeda-Kamiya N, Magome H, Kamiya Y, Shirasu K, Yoneyama K. 2008. Inhibition of shoot branching by new terpenoid plant hormones. *Nature* 455: 195–200.
- Wang F, Han T, Song Q, Ye W, Song X, Chu J, Li J, Chen ZJ. 2020. The rice circadian clock regulates tiller growth and panicle development through strigolactone signaling and sugar sensing. *Plant Cell* 32: 3124–3138.
- Wang Q, Ni J, Shah F, Liu W, Wang D, Yao Y, Hu H, Huang S, Hou J, Fu S. 2019. Overexpression of the stress-inducible SsMAX2 promotes drought and salt resistance via the regulation of redox homeostasis in *Arabidopsis*. *International Journal of Molecular Sciences* 20: 837.
- Wang Y, Duan G, Li C, Ma X, Yang J. 2021. Application of jasmonic acid at the stage of visible brown necrotic spots in *Magnaporthe oryzae* infection as a novel and environment-friendly control strategy for rice blast disease. *Protoplasma* 258: 743–752.
- Wasternack C, Hause B. 2013. Jasmonates: biosynthesis, perception, signal transduction and action in plant stress response, growth and development. An update to the 2007 review in *Annals of Botany*. *Annals of Botany* 111: 1021–1058.
- Wasternack C, Strnad M. 2018. Jasmonates: News on occurrence, biosynthesis, metabolism and action of an ancient group of signaling compounds. *International Journal of Molecular Sciences* 19: 2539.
- Xi L, Wen C, Fang S, Chen X, Nie J, Chu J, Yuan C, Yan C, Ma N, Zhao L. 2015. Impacts of strigolactone on shoot branching under phosphate starvation in chrysanthemum (*Dendranthema grandiflorum* cv. Jinba). *Frontiers in Plant Science* 6: 694.
- Xu J, Wang X, Zu H, Zeng X, Baldwin IT, Lou Y, Li R. 2021. Molecular dissection of rice phytohormone signaling involved in resistance to a piercing-sucking herbivore. *New Phytologist* 230: 1639–1652.
- Xu X, Fang P, Zhang H, Chi C, Song L, Xia X, Shi K, Zhou Y, Zhou J, Yu J. 2019. Strigolactones positively regulate defense against root-knot nematodes in tomato. *Journal of Experimental Botany* 70: 1325–1337.
- Yang D-L, Yao J, Mei C-S, Tong X-H, Zeng L-J, Li Q, Xiao L-T, Sun T-p, Li J, Deng X-W. 2012. Plant hormone jasmonate prioritizes defense over growth by interfering with gibberellin signaling cascade. *Proceedings of the National Academy of Sciences, USA* 109: E1192–E1200.
- Yara A, Yaeno T, Hasegawa M, Seto H, Seo S, Kusumi K, Iba K. 2008. Resistance to *Magnaporthe grisea* in transgenic rice with suppressed expression of genes encoding allene oxide cyclase and phytyldienoic acid reductase. *Biochemical and Biophysical Research Communications* 376: 460–465.
- Yoneyama K, Xie X, Kim HI, Kisugi T, Nomura T, Sekimoto H, Yokota T, Yoneyama K. 2012. How do nitrogen and phosphorus deficiencies affect strigolactone production and exudation? *Planta* 235: 1197–1207.
- Zhang X, Bao Y, Shan D, Wang Z, Song X, Wang Z, Wang J, He L, Wu L, Zhang Z *et al.* 2018. *Magnaporthe oryzae* induces the expression of a microRNA to suppress the immune response in rice. *Plant Physiology* 177: 352–368.
- Zheng J, Hong K, Zeng L, Wang L, Kang S, Qu M, Dai J, Zou L, Zhu L, Tang Z *et al.* 2020. Karrikin signaling acts parallel to and additively with strigolactone signaling to regulate rice mesocotyl elongation in darkness. *Plant Cell* 32: 2780–2805.

## Supporting Information

Additional Supporting Information may be found online in the Supporting Information section at the end of the article.

**Fig. S1** Lesion score distribution in rice strigolactone-mutants and wild-type plants infected by *Pyricularia oryzae*.

**Fig. S2** *In vitro* bioassay with *Pyricularia oryzae* using the strigolactone inhibitor TIS108.

**Fig. S3** Concentrations of jasmonates in rice leaves after treatment with the strigolactone analog *rac*-GR24.

**Fig. S4** Complementation of the strigolactone biosynthetic mutant *d10* by *rac*-GR24 treatment.

**Fig. S5** Soluble sugar content in rice leaves after *rac*-GR24 treatment.

**Fig. S6** Concentrations of reactive oxygen species in rice strigolactone-mutants and TIS108-treated plants.

**Fig. S7** Concentrations of reactive oxygen species in rice seedlings after treatment with the strigolactone analog *rac*-GR24.

**Fig. S8** Jasmonate levels in rice mutants defective in JA-Ile synthesis (*jar1*) and jasmonate perception (*coi1-18* RNAi).

**Fig. S9** Accumulation of jasmonates in rice leaves after treatment with methyl jasmonate.

**Fig. S10** Effect of methyl jasmonate treatment on the accumulation of soluble sugars in rice.

**Table S1** Chromatographic gradient for analysis of jasmonates by LC–MS/MS.

**Table S2** Details of analysis of jasmonates by LC–MS/MS.

**Table S3** Chromatographic gradient for analysis of flavonoid phytoalexins by LC–MS/MS.

**Table S4** Details of analysis of flavonoid phytoalexins by LC–MS/MS.

**Table S5** Chromatographic gradient for analysis of soluble sugars by LC–MS/MS.

**Table S6** Details of analysis of soluble sugars by LC–MS/MS.

**Table S7** Primer sequences used in this study for RT-qPCR.

**Table S8** Statistical results of a two-way ANOVA for the levels of hormone metabolites in rice leaves infected with the blast fungus *Pyricularia oryzae*.

**Table S9** Statistical results of a two-way ANOVA for the levels of sugar metabolites in *Pyricularia oryzae*-infected rice leaves.

**Table S10** Statistical results of a two-way ANOVA for the transcripts of strigolactone genes.

**Table S11** Statistical results of a two-way ANOVA for the levels of flavonoid metabolites in rice leaves infected with the blast fungus *Pyricularia oryzae*.

**Table S12** Statistical results of a two-way ANOVA for *Pyricularia oryzae*-infected strigolactone-mutant lines with and without *rac*-GR24 pretreatment.

**Table S13** Statistical results of a two-way ANOVA for *Pyricularia oryzae*-infected JA-mutant lines with and without strigolactone inhibition.

Please note: Wiley is not responsible for the content or functionality of any Supporting Information supplied by the authors. Any queries (other than missing material) should be directed to the *New Phytologist* Central Office.